Unclassified
SECURITY CLASSIFICATION OF THIS PAGE

DTIC FILE COPY (4)

REPORT DOCUMENTATION PAGE

Form Approved OMB No. 0704-0188

AD-A192 440

	1b. RESTRICTIVE MARKINGS: N/A
N/A	3. DISTRIBUTION/AVAILABILITY OF REPORT: This document has been approved for public release and sale; its distribution is unlimited.
4. PERFORMING ORGANIZATION REPORT NUMBER(S): None	5. MONITORING ORGANIZATION REPORT NUMBER(S)
6a. NAME OF PERFORMING ORGANIZATION: Pinnacle Research Inst. / 6b. OFFICE SYMBOL (If applicable): N/A	7a. NAME OF MONITORING ORGANIZATION: Office of Naval Research, Department of the Navy
6c. ADDRESS (City, State, and ZIP Code): 10432 N. Tantau Ave., Cupertino, CA 95014	7b. ADDRESS (City, State, and ZIP Code): 800 N. Quincy Street, Arlington, Virginia 22217-5000
8a. NAME OF FUNDING/SPONSORING ORGANIZATION: Strategic Defense Initiative Org. / 8b. OFFICE SYMBOL (If applicable): SDIO	9. PROCUREMENT INSTRUMENT IDENTIFICATION NUMBER: N00014-87-C-0705
8c. ADDRESS (City, State, and ZIP Code): The Pentagon, Washington, DC 20301-7100	10. SOURCE OF FUNDING NUMBERS: PROGRAM ELEMENT NO. / PROJECT NO. / TASK NO. / WORK UNIT ACCESSION NO.

DTIC ELECTE MAR 15 1988 S D

11. TITLE (Include Security Classification): HIGH POWER PULSE ENERGY SYSTEM CONCEPT

12. PERSONAL AUTHOR(S): LEE, Ho-Lun; MASON, Gary; KERN, Kurt

13a. TYPE OF REPORT	13b. TIME COVERED	14. DATE OF REPORT (Year, Month, Day)	15. PAGE COUNT
Final	FROM 87-9-1 TO 89/2/28	1988 Feb 22	51

16. SUPPLEMENTARY NOTATION: N/A

17. COSATI CODES		
FIELD	GROUP	SUB-GROUP

18. SUBJECT TERMS (Continue on reverse if necessary and identify by block number): Pulse energy; Burst power; Battery; Capacitor; High energy density; Electrochemical capacitor; Ultracapacitor.

19. ABSTRACT (Continue on reverse if necessary and identify by block number)

New advances in capacitor technology create exciting opportunities in size and weight reduction for high-power, pulse energy systems having a broad range of applications. Characteristics of a proposed high power pulse energy system, formed by combining a recently developed, high-energy density capacitor with various batteries, were investigated. Main advantages of the system thus far appear to be high power and pulse energy density and flexibility in energy outputs. Parametric relationships between most key design variables, such as average pulse power, system output voltages, load impedance, pulse width, pulse frequency, duty cycle and battery's voltage and current limits, were established. Projections of the system's weights in large-scale applications suggested that the lithium/SO_2 battery considered might be too heavy when high duty cycles were required. However, significant weight reductions could be foreseen with proper selection of the battery and further advances in the capacitor technology. Keywords: Lithium Sulfur Dioxide Battery;

20. DISTRIBUTION/AVAILABILITY OF ABSTRACT	21. ABSTRACT SECURITY CLASSIFICATION
☒ UNCLASSIFIED/UNLIMITED ☐ SAME AS RPT. ☐ DTIC USERS	Unclassified
22a. NAME OF RESPONSIBLE INDIVIDUAL	22b. TELEPHONE (Include Area Code) / 22c. OFFICE SYMBOL

DD Form 1473, JUN 86 — Previous editions are obsolete. — SECURITY CLASSIFICATION OF THIS PAGE

Unclassified

Best
Available
Copy

OFFICE OF NAVAL RESEARCH

Contract N00014-87-C-0705

R & T Code S405023SRA01

Technical Report No. 2

High Power Pulse Energy System Concept

by

Ho-Lun Lee, G. Mason, K. Kern

Prepared in Fulfillment of Subline Item 0001AC,

"Final Technical Report"

as Required by the Contract

Pinnacle Research Institute
10432 N. Tantau Avenue
Cupertino, CA 95014

February 22, 1988

Reproduction in whole or in part is permitted
for any purpose of the United States Government.

This document has been approved for public release
and sale; its distribution is unlimited.

88 3 15 010

TABLE OF CONTENTS

Accesion For
NTIS CRA&I
DTIC TAB
Unannounced
Justification
By
Distribution/
Availability Codes
Dist | Avail and / or Special
A-1

Summary

The melding of state of the art capacitor and battery technology has been demonstrated to result in a hybrid pulse power system exhibiting many desirable characteristics. In particular the use of a high energy and power density capacitor recently developed can provide multiple bursts of energy at high power before requiring recharge, thus reducing the power requirement on the battery in certain applications. In the extreme case, a capacitor can be developed to store enough energy to meet all burst power requirements, and only a low power battery will be needed to replenish the charge lost in the capacitor due to leakage current.

The hybrid pulse power system has been characterized thoroughly to establish the parametric relationships between duty cycle, power, pulse width, load resistance, operating voltages of the capacitor and the battery, and current capability of the battery. These relationships are mostly in the form of correlations, although a simple model is found to describe the system behavior quite well at low duty cycles and pulse widths. These results have then been used to project and optimize system performances in some hypothetical applications.

Complete characterization of hybrid pulse power systems, however, has been hampered by inadequate equipment and time. Thus it has not been possible to examine the application involving duty cycles with multiple power bursts followed by

charging of the capacitor, or systems having as their primary energy source batteries other than the lithium/SO_2 cells utilized in our investigation thus far. Nevertheless it has become clear that the lithium nonaqueous battery has relatively low current density (5 MA/cm^2) and may be unsuitable for high duty cycle, burst power applications.

Some projections have been made for the performance of the hybrid pulse power system. Depending on the duty cycle and energy requirements of the application, power density as high as 800 kW/kg and energy density approaching that of lithium batteries (0.5 kwh/kg) are achievable, but would require careful design and optimization of the system components and their parameters.

I. CONSTRUCTION OF THE ULTRACAPACITOR

A 36V, 0.3F ultracapacitor was fabricated using technology developed at Pinnacle Research Institute under DOD funding. Detailed construction of the device is illustrated in Figure 1 and a picture of it is shown in Figure 2. The capacitor consists basically of a stack of thin titanium electrode disks, separated by glass fibrous papers in the middle and thin rings of viton gaskets along their circumferences. Each electrode is coated on both sides by a proprietary material which is a mixed metal oxide to account for its charge storage capacity. Sulfuric acid is used as an electrolyte which is imbibed by the glass fibrous separator and also fills the interelectrode gaps. The active volume of the device is calculated to be 10.3 cc, based on an active area of 14.6 cm^2 (1.7 in. dia.) and a stack height of 0.704 cm. Internal impedance of the device was measured with a GenRad Digibridge to be 70 mohms at 1 kHz, and the leakage current was 5.3 mA at full charge. This capacitor was designed to provide a maximum output power of 3.2 kW with minimal size.

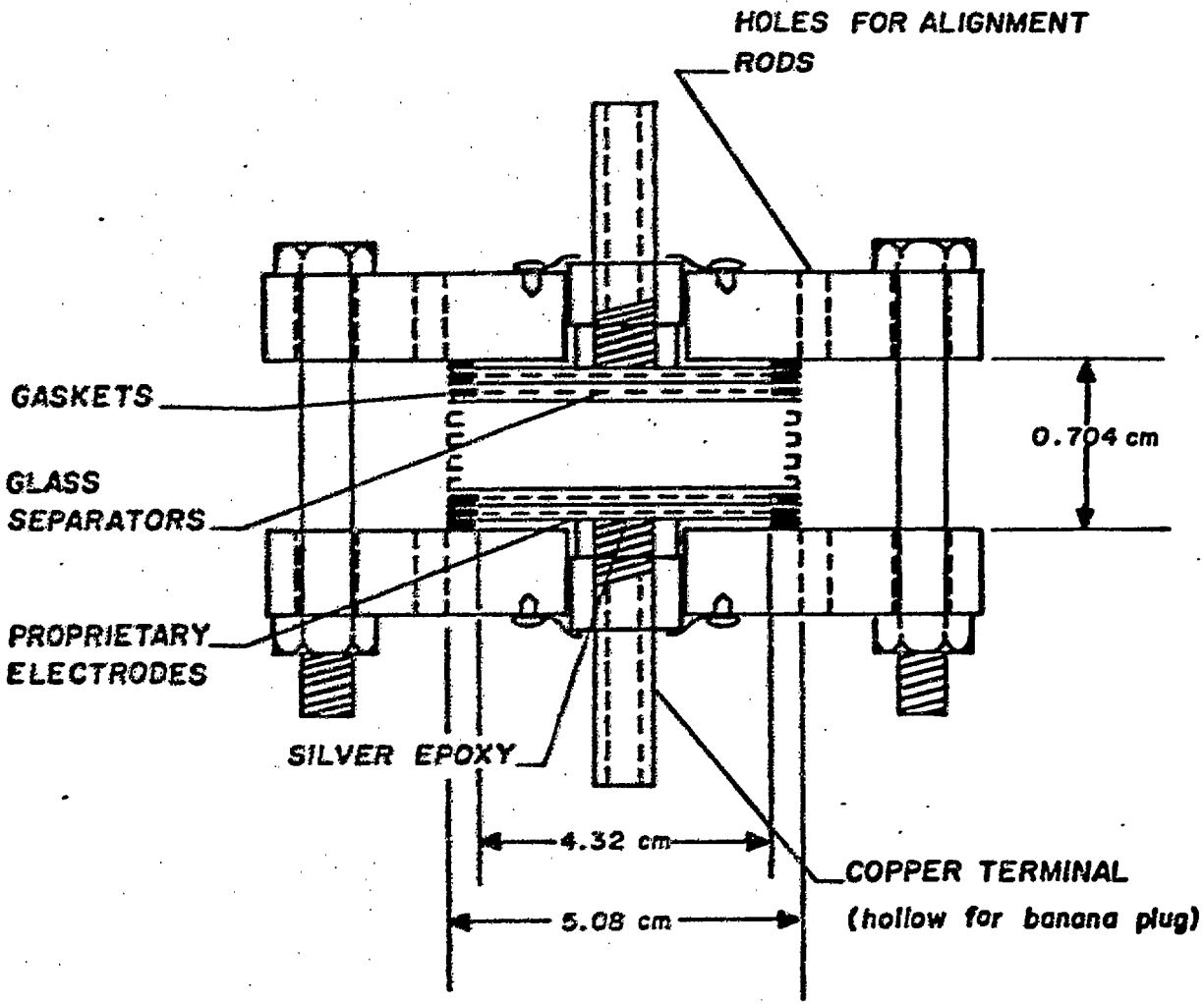

Figure 1. Design of the Experimental Ultracapacitor for 1 to 3 kW Pulse Power Applications

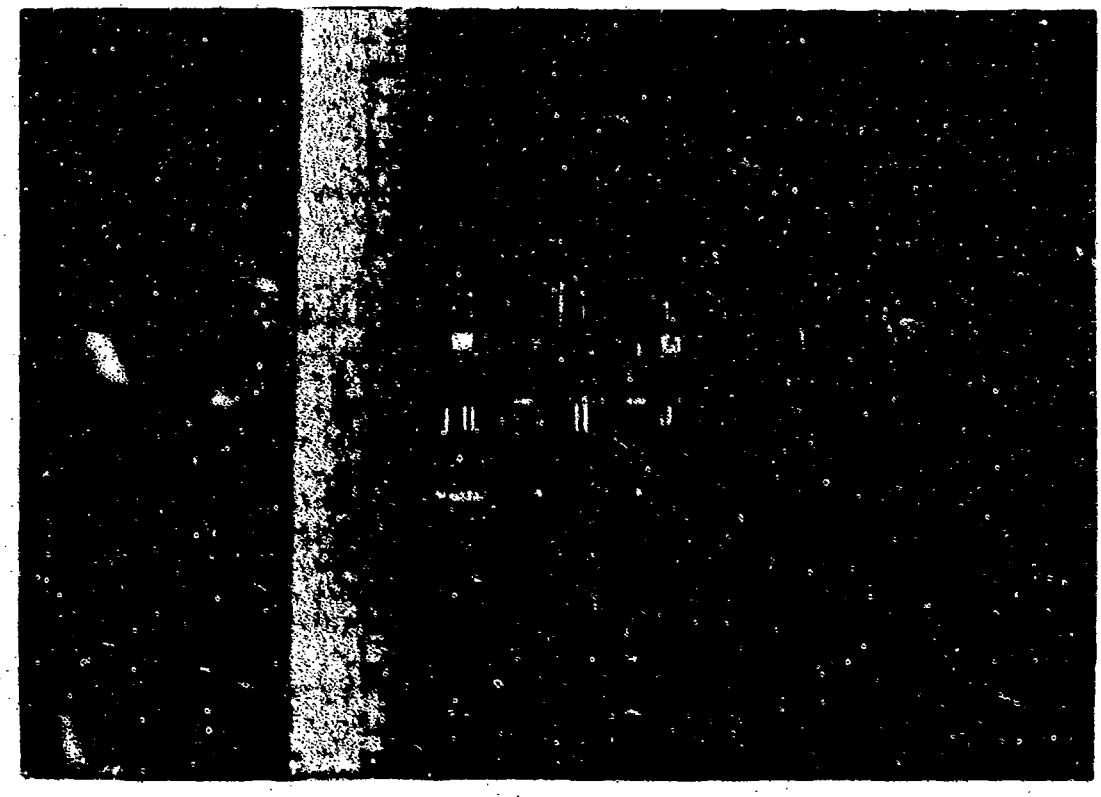

Figure 2. A Photograph of the Ultracapacitor constructed for the Hybrid Pulse Power System

II. DISCHARGE CHARACTERISTICS OF THE ULTRACAPACITOR

Discharge experiments were conducted with a pulse tester fabricated in house (Fig. 3). The test circuitry consisted primarily of a parallel arrangement of FET switches, which were activated by a voltage signal from a "clocked" power supply. The timing mechanism was electronic to permit rapid changes, down to 0.1 msec, in the voltage from the power supply. Data, in the form of voltage and current, were collected with oscilloscopes. A digital oscilloscope was used for maximum data accuracy, but an analog oscilloscope was sometimes preferred for variable time intervals of data sampling, as required when the pulses were spaced far apart.

A. Characteristics of a Single Pulse

A typical discharge pulse of the ultracapacitor across a constant resistive load is as shown in Fig. 4. The maximum power output is accompanied by a rapid drop in voltage, followed by a more gradual decline along a constant RC discharge curve. The time constant for this latter portion of the voltage decay suggests an effective capacitance of 0.076F for the capacitor, still considerably less than the capacitance for charge storage in this device. This anomaly is at present not well understood, but ongoing research with AC Impedance technique is expected to shed some lights on this intriguing subject.

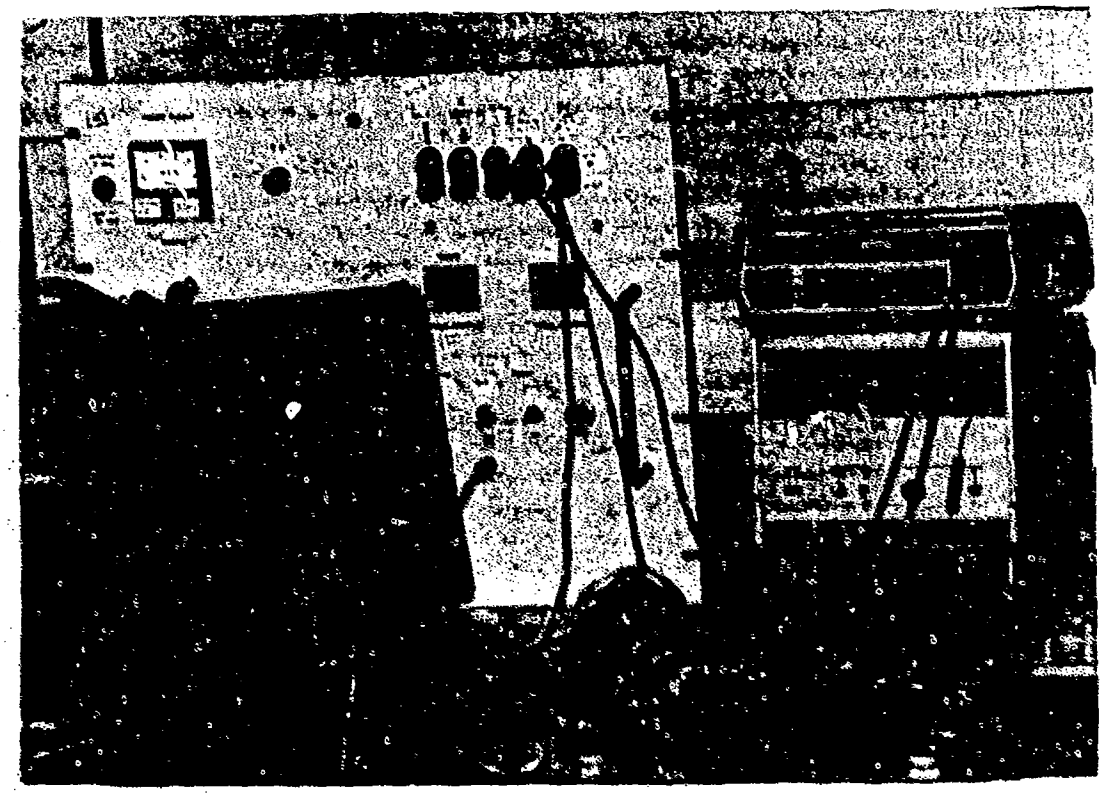

Figure 3. Experimental Setup for the pulse testing of Capacitors

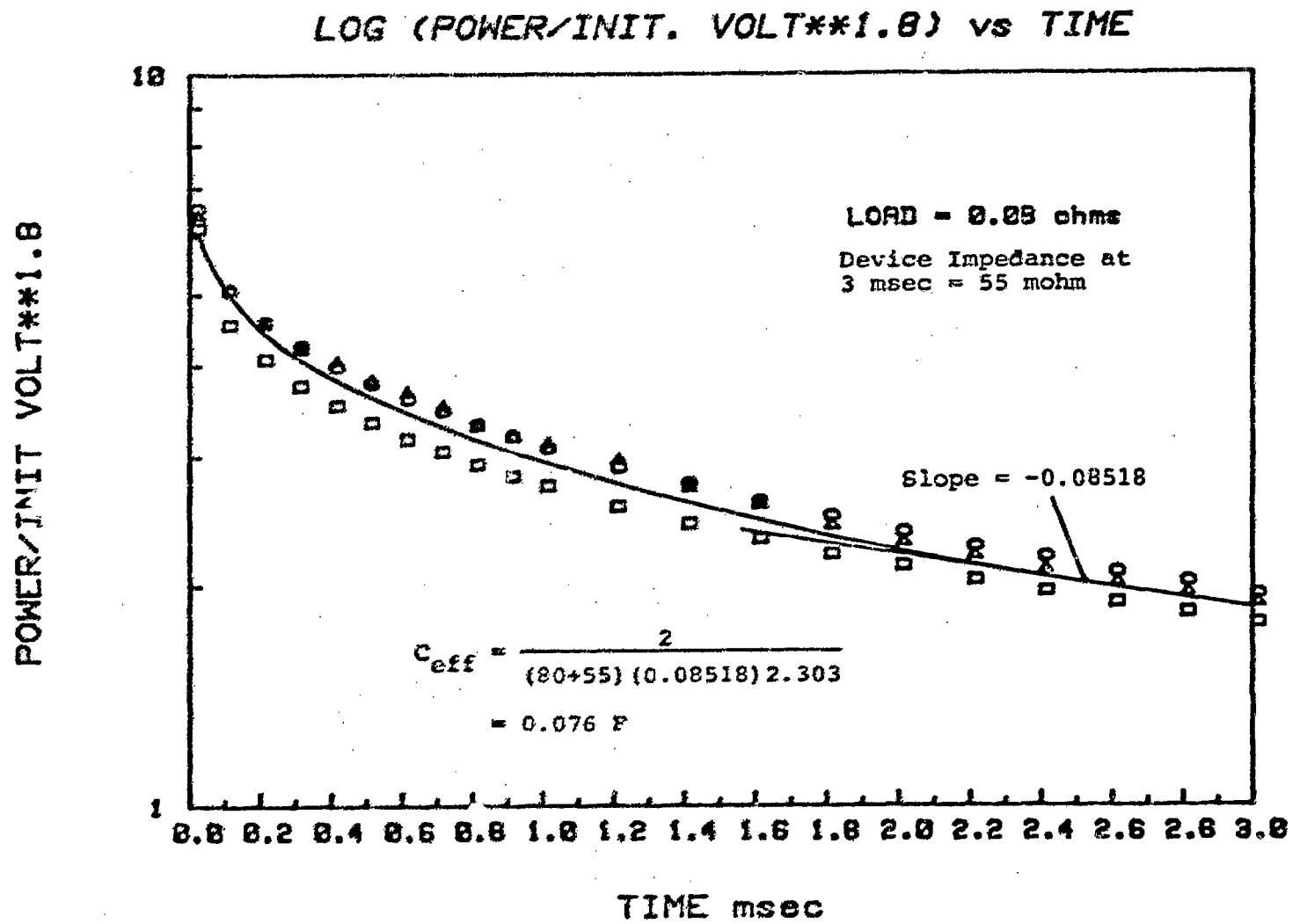

Figure 4. Discharge power of the Ultracapacitor across a constant load at 0.08 ohm, matching the internal impedance of the device.

The discharge of the ultracapacitor behaves much like one whose capacitance varies with time due to some internal transient. For a long-duration discharge, the effective capacitance C_{eff}, defined as

$$C_{eff} = \frac{i}{\frac{dV}{dt}} = \frac{2}{R\,\frac{d\ln P}{dt}} \qquad (1)$$

where P is power, V is open circuit voltage, i is current and R is the total circuit resistance, approaches the capacitance for charge storage asymptotically. Further, the time dependent C_{eff} is not significantly affected by the rate at which the capacitor is discharged, as suggested by a comparison of the results shown in Fig. 5 with those in Fig. 4. Figure 4 gives a C_{eff} of 0.076F after 3 msec whereas Figure 5 gives C_{eff} of 0.063F, not significantly different. In addition, C_{eff} does not vary significantly with the initial voltage of the discharge.

The observation that the power is proportional to initial open circuit voltage (OCV) on the capacitor to the 1.8th power rather than the 2nd could be explained by a voltage-dependent internal impedance for the ultracapacitor, as shown in Fig. 6. The results presented were obtained from the initial measured power, at 10 μsec, and the assumption of no change in OCV for the first 10 μsec of discharge.

Following a discharge, the OCV of the ultracapacitor typically increases somewhat for a short time period. This voltage recovery remains to be further investigated in a future research program.

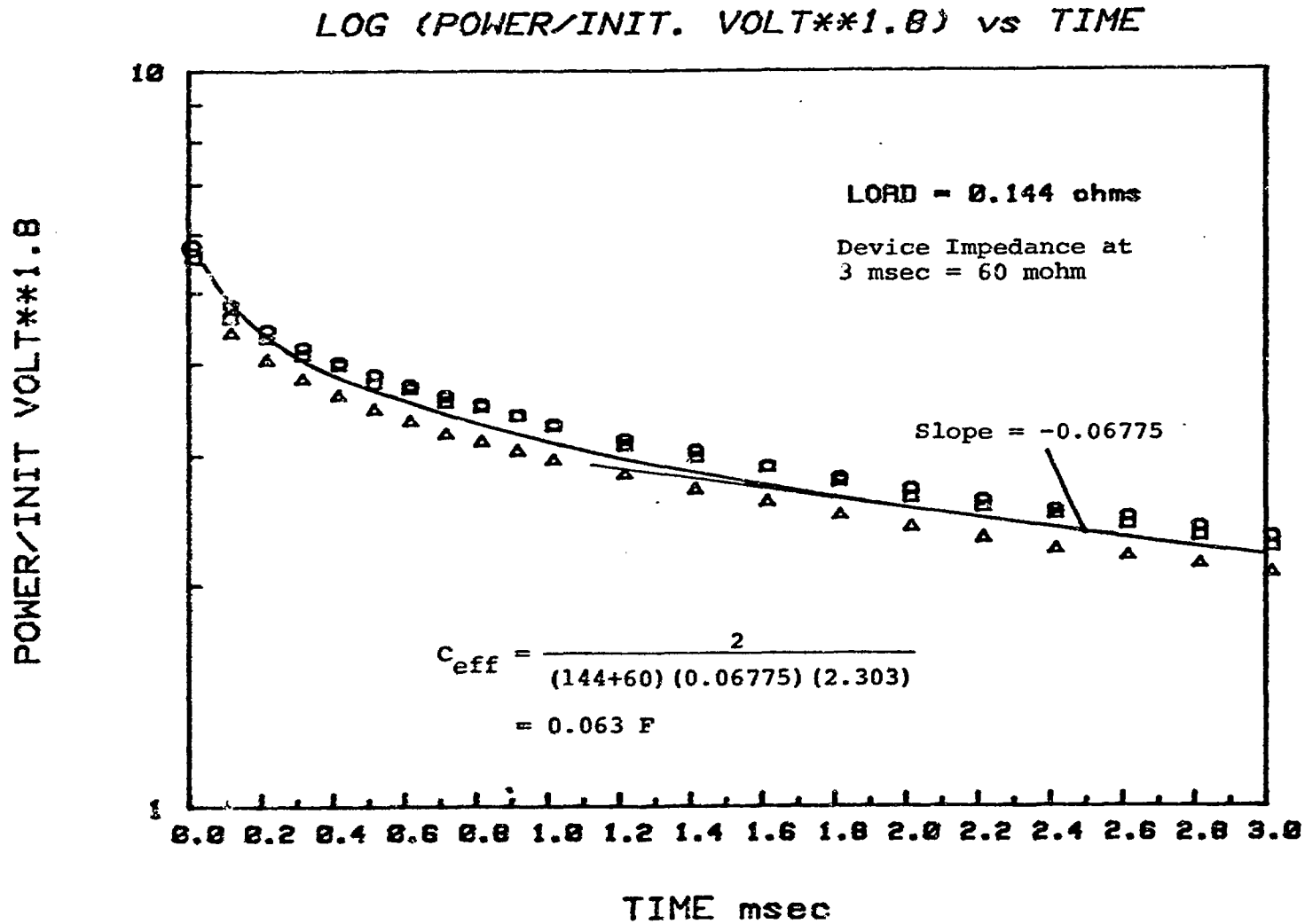

Figure 5. Discharge power of the Ultracapacitor across a constant load at 0.144 ohm.

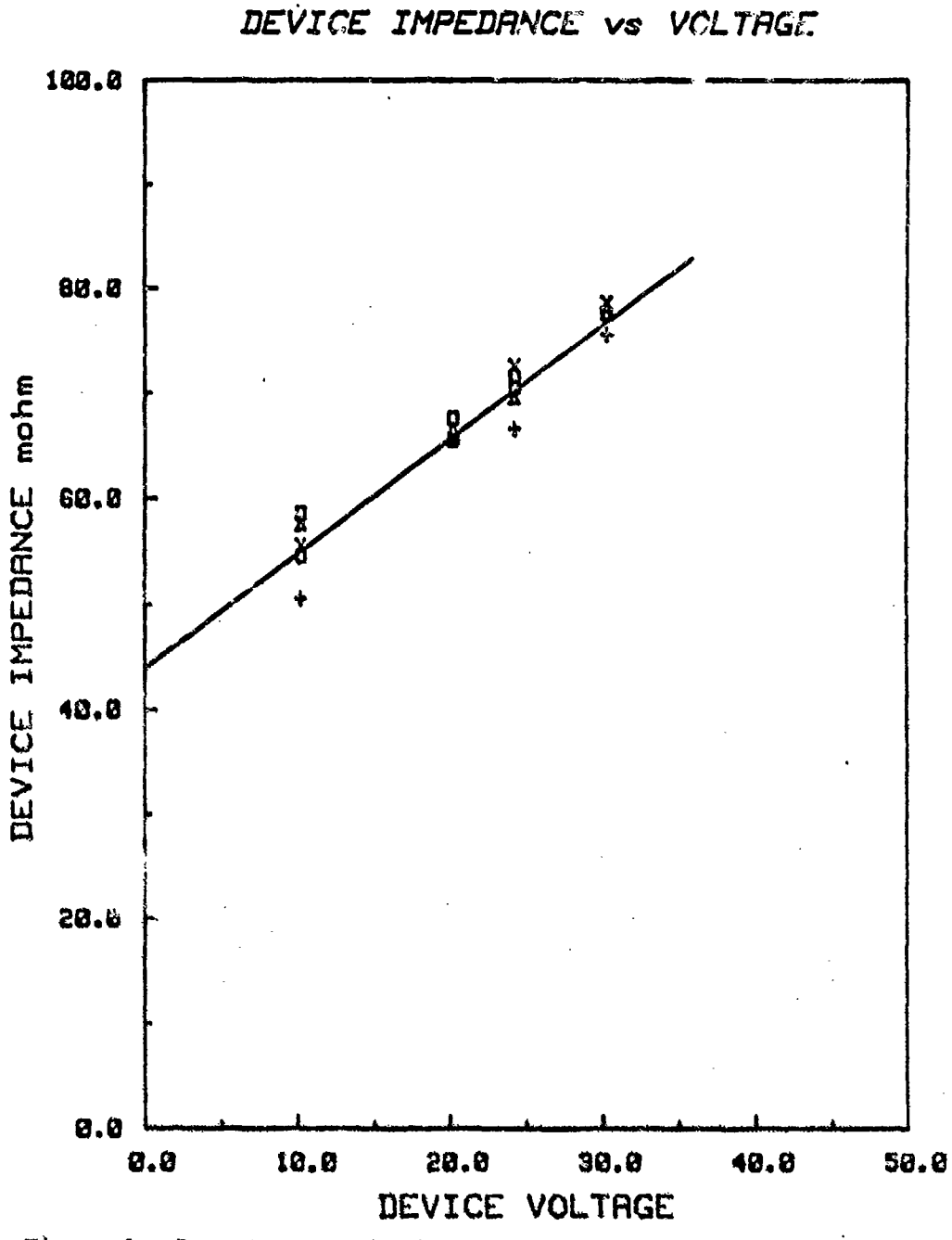

Figure 6. Dependence of the internal impedance of the Ultracapacitor on its open circuit voltage.

Perhaps of greater interest here is the average power in a pulse, and this is summarized in Fig. 7. The average power increases as the pulse duration shortens, and also can be maximized by selecting the proper load resistance, which is generally larger than the internal impedance of the capacitor. The highest average power that can be obtained for a 3 msec pulse is about 1.37 kW. Therefore the burst energy per pulse is 4.1 J, only 2.8% of the total stored energy. The pulse energy density of our ultracapacitor is thus 0.4 MJ/M^3, still compared favorably with energy densities of other types of capacitors (e.g. electrolytic has about 0.1 MJ/M^3). By extrapolating to larger pulse width, higher pulse energy density can be obtained. For example Fig. 8 shows that with a 10 msec pulse, the energy density becomes 1.1 MJ/M^3 as calculated from the graph. In addition, given the same battery power and space available for capacitors, our ultracapacitor can provide the burst mode as shown in Fig. 9 and is thus much more versatile. This feature is more clearly illustrated by results reported below.

B. Characteristics of Pulse Trains

With the pulse tester shown previously in Fig. 3, series of current pulses were produced from our ultracapacitor with energy stored from a single cycle of charging, as follows. The capacitor was first charged to 30 V, then pulse discharged across a 0.08 ohm load with variable pulse intervals, i.e.

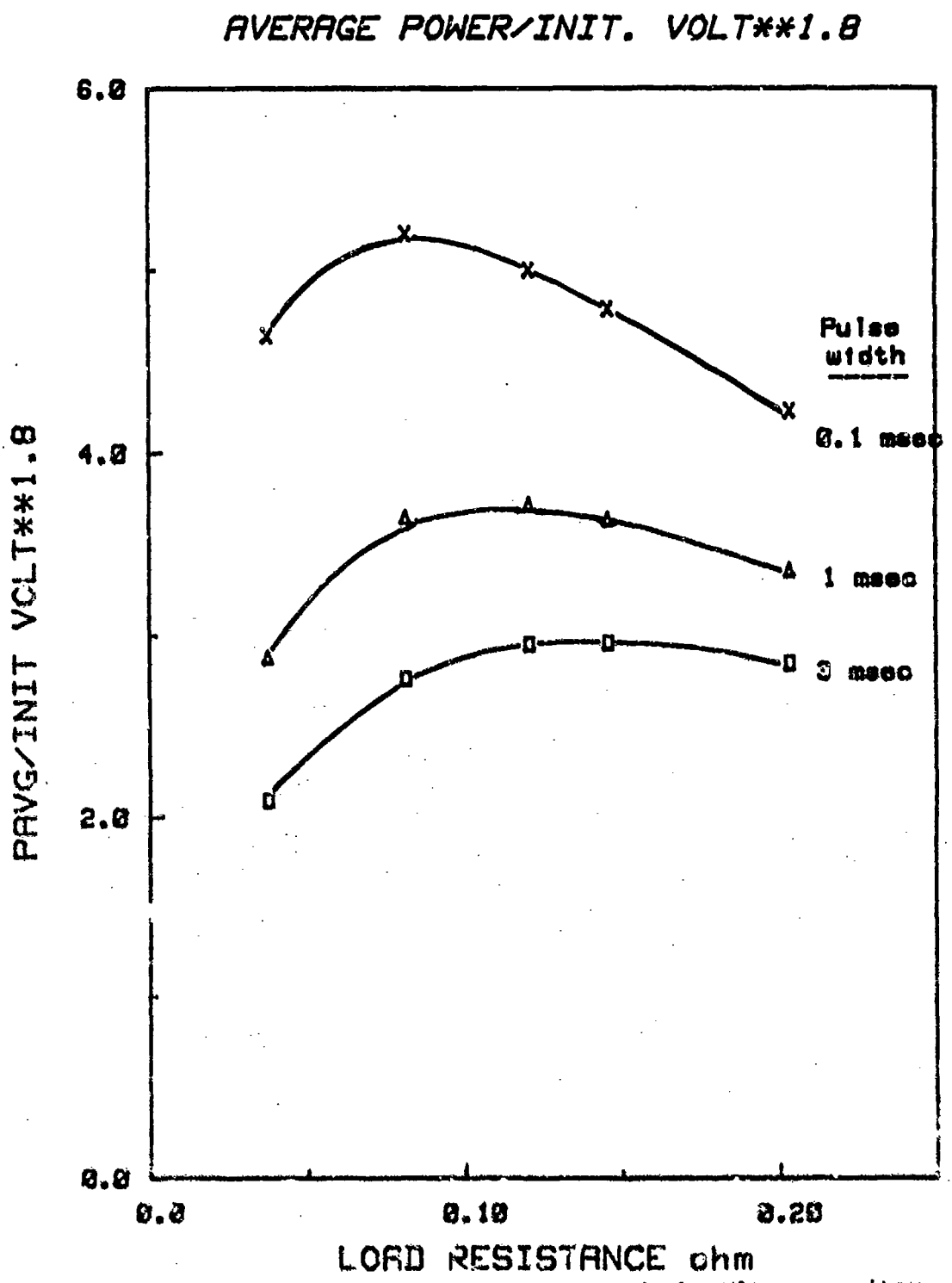

Figure 7. Average pulse-discharge power of the Ultracapacitor as a function of load resistance for several pulse durations.

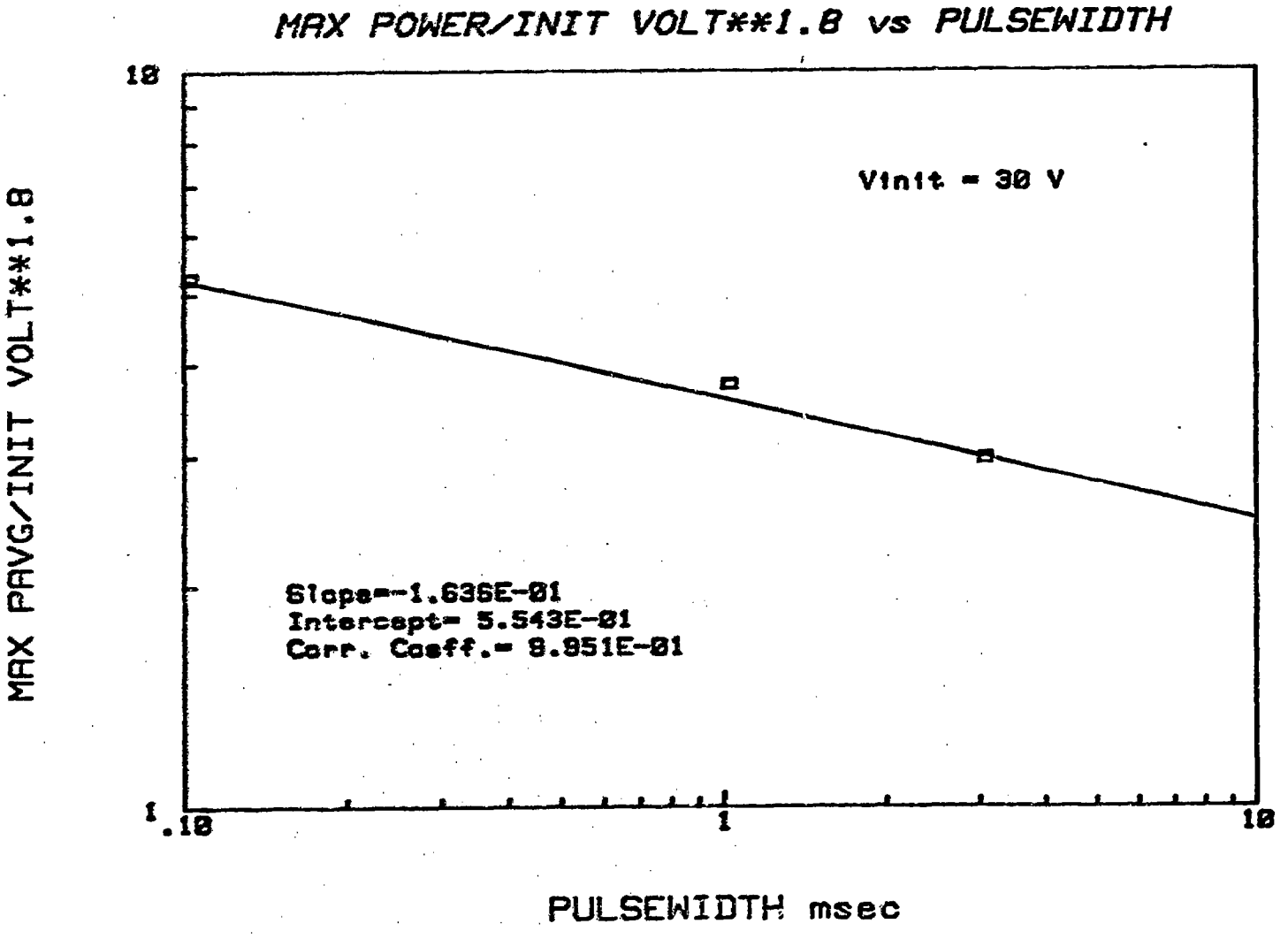

Figure 8. Maximum average power in a pulse from the Ultracapacitor as a function of pulse duration.

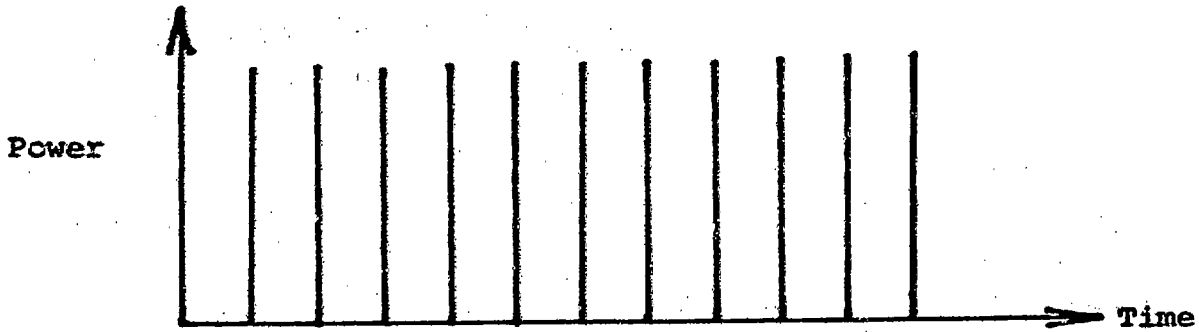

(a) Burst mode with conventional capacitors

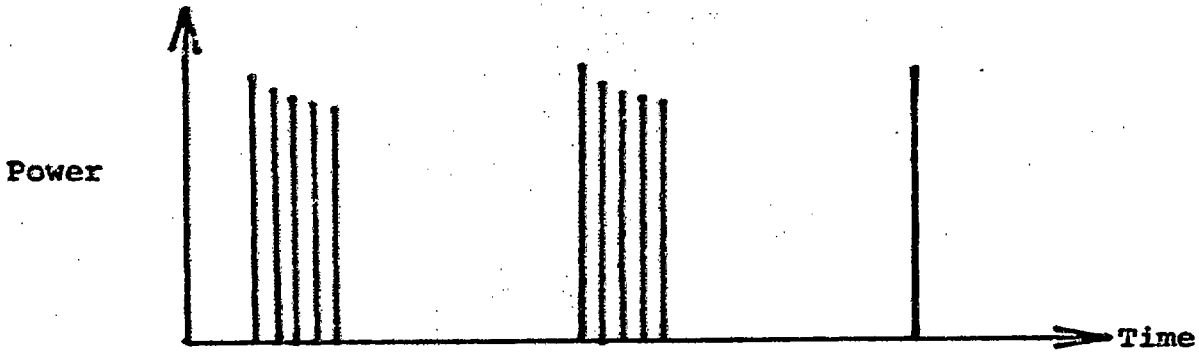

(b) Alternate burst mode with Ultracapacitors

Figure 9. Comparison of burst modes from different capacitors.
(a) conventional (b) &(a) with Ultracapacitor

rest time between successive pulses, and pulse widths.

Due to limitations of the oscilloscope, only one pulse could be recorded for every discharge experiment. Hence to examine a series of fifteen pulses, fifteen identical discharge experiments had to be performed.

Results obtained are highlighted in Fig. 10 and 11. It can be seen that the rate of relative power loss is highest for the initial pulse, and becomes considerably less thereafter. The fractional change in power after every pulse can also be reduced by increasing rest intervals between pulses, as a consequence of the voltage recovery phenomenon alluded to earlier. On the whole, an average power level of approximately 1 kW can be sustained for a series of 15 pulses with the present ultracapacitor. Variable load resistance could be employed if truly uniform power were desired from pulse to pulse.

An intrinsic power density of about 100 MW/M^3 could therefore be realized for a series of fifteen 1 msec pulses. In addition, such short bursts of energy could be released with variable time intervals in between without regard to the charging power of the battery.

The only practical limit on this unique capability of the ultracapacitor is the P/E ("burst" power to total energy) ratio of the specific application for the pulse energy system. Where the P/E is less than that of the ultracapacitor, presently at 6.7 sec^{-1} at peak power, more than a single charge of the

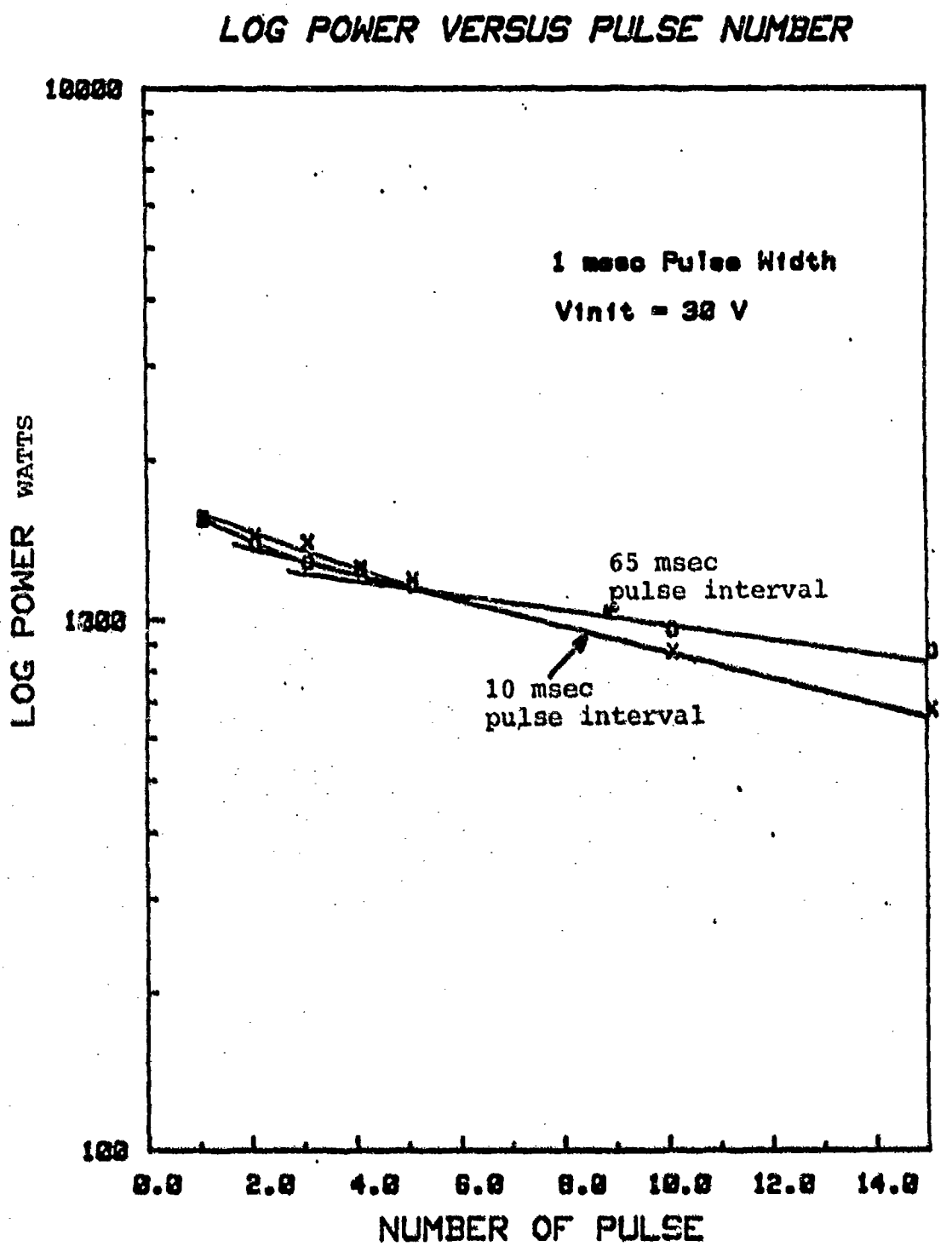

Figure 10. Average pulse power in a series of fifteen 1 msec pulses

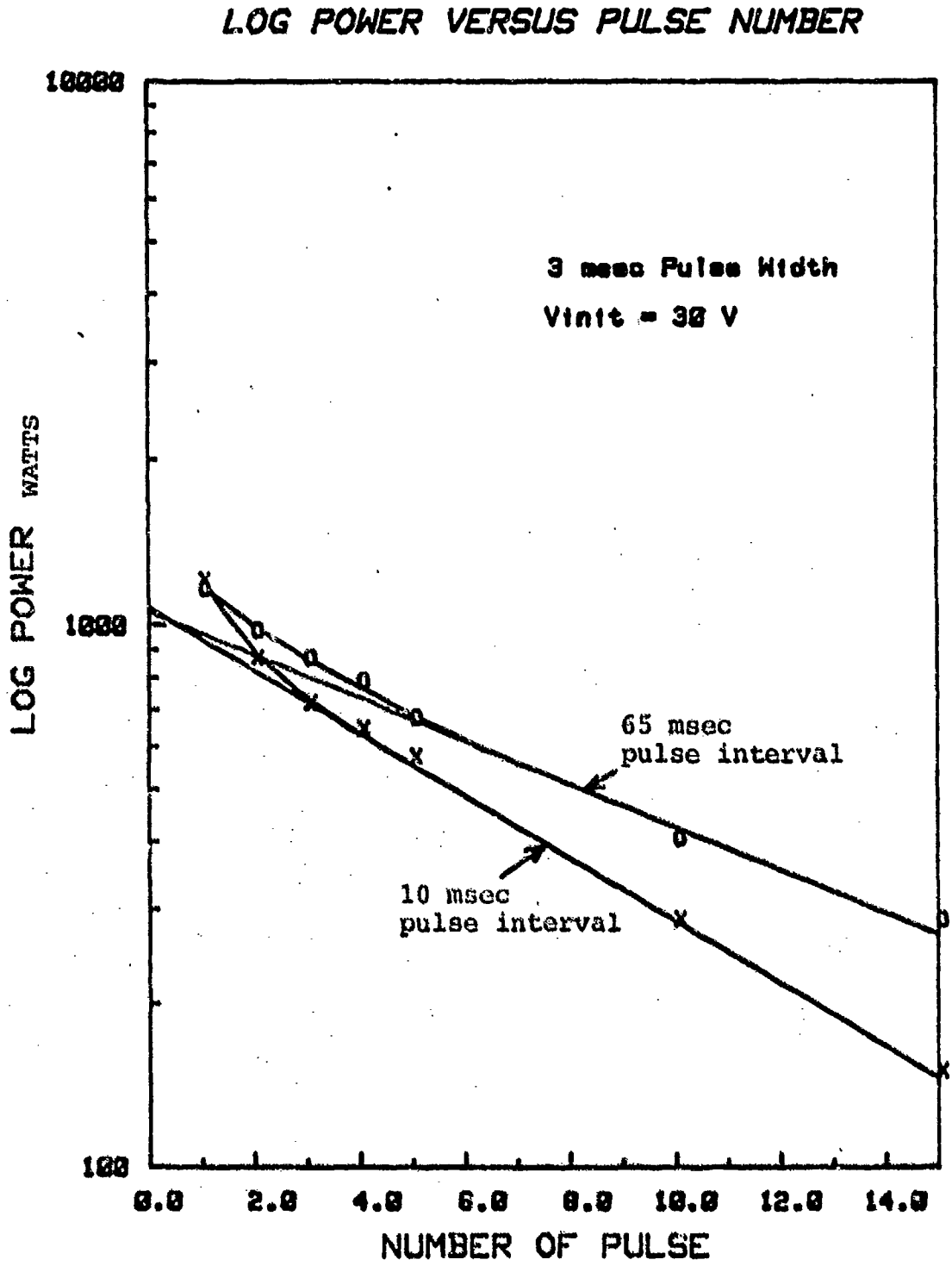

Figure 11. Average pulse power in a series of fifteen 3 msec pulses

ultracapacitor is required. The flexibility afforded by variable pulse intervals is then possible only within a duty cycle but the period of the cycle is bounded from below by the minimum time to charge with the battery.

Comparison of Fig. 10 and 11 shows that the average power from three 1 msec pulses is higher than the average power from one 3 msec pulse. Hence the "burst" power density can be optimized for specific applications. Furthermore since the average power decreases as more energy is extracted from the capacitor per duty cycle, there is a compromise between useful power and energy density for this power component.

In Fig. 12, the pulse power density of our present ultracapacitor is plotted against the useful energy density for a duty cycle. The latter parameter may be significant in that it is the total burst energy which can be released at a faster rate than the discharge rate of the battery. It can be seen that the useful energy density generally increases at the expense of the pulse power density, but appears to approach various limiting values depending on the pulse width and interval. Practically these limits would never be reached since, once the power density of the ultracapacitor fell below that of the battery, power conditioning through the capacitor would no longer be required.

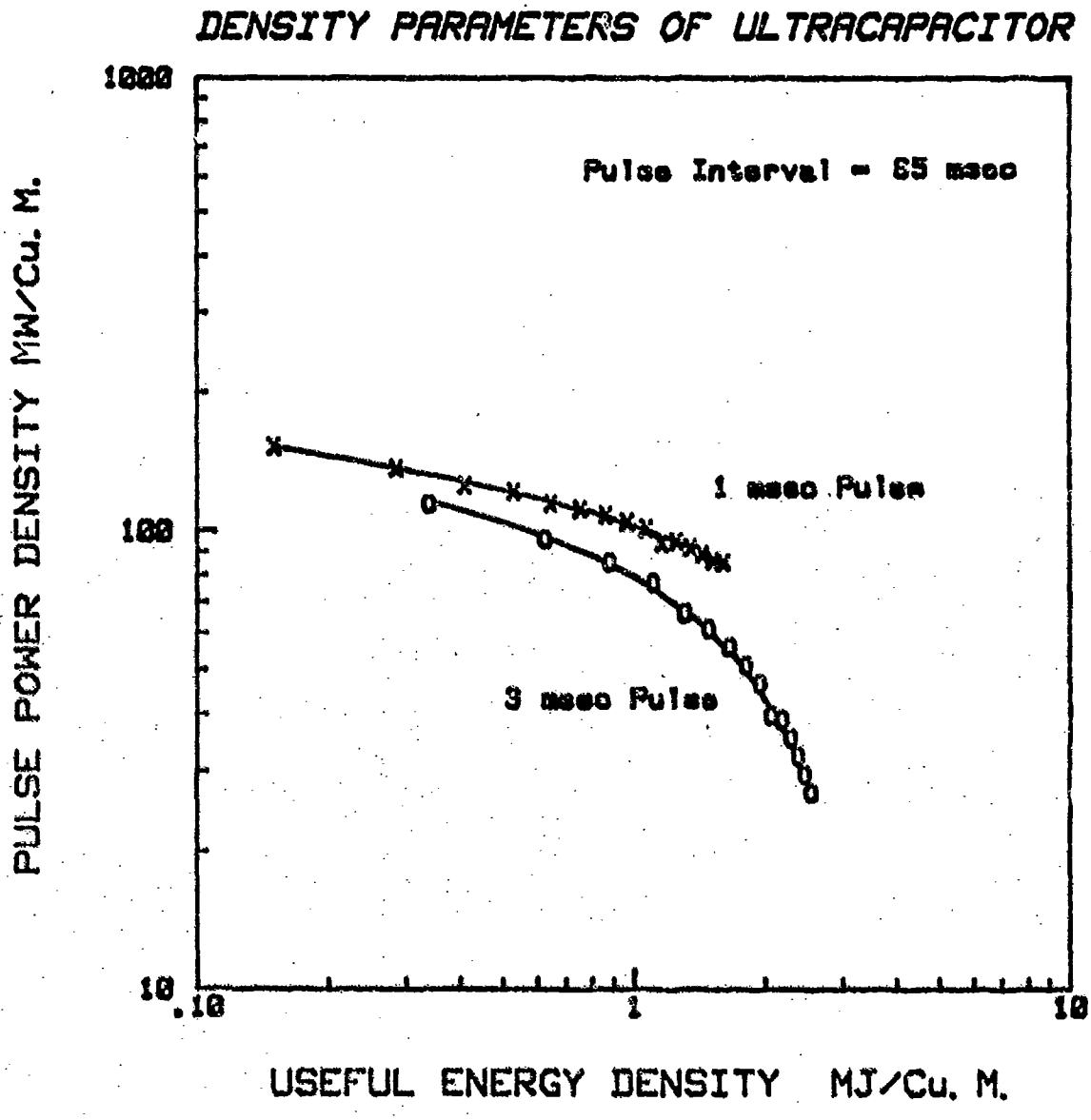

Figure 12. Trade-offs between useful power and energy densities for the Ultracapacitor as the number of pulses in a duty cycle increases.

The observation of a smaller pulse width leading to greater power for the same useful energy output is believed to be generally true. The reason is that the energy which is released early in a pulse discharge is stored in the more readily accessible sites in the ultracapacitor electrodes, hence giving higher power due to a faster rate of release. After a discharge, energy is redistributed evenly amoung all sites in a recovery period. This redistribution effectively increases the power density of the ultracapacitor. With pulses of shorter duration, less energy is expended per pulse. Therefore the stored energy is allowed to redistribute more frequently before it is released, and the derived power is greater.

To pursue this important finding further, series of pulses with 0.1 msec duration were examined. As shown in Figure 13, average pulse power after 100 pulses remained quite high, corresponding to a power density of 134 MW/M^3 for our ultracapacitor. The useful energy density at this point was calculated to be 1.6 MJ/M^3. In comparison the power density of a series of 1 msec pulses had fallen to less than 100 MW/M^3 after the same amount of energy was delivered.

Another important observation seemed to be that in spite of the frequent on/off switching of our ultracapacitor, as with the 0.1 msec pulse series, no significant loss in power or useful energy density could be discerned. A single charge of our ultracapacitor could produce a great number of pulses, provided

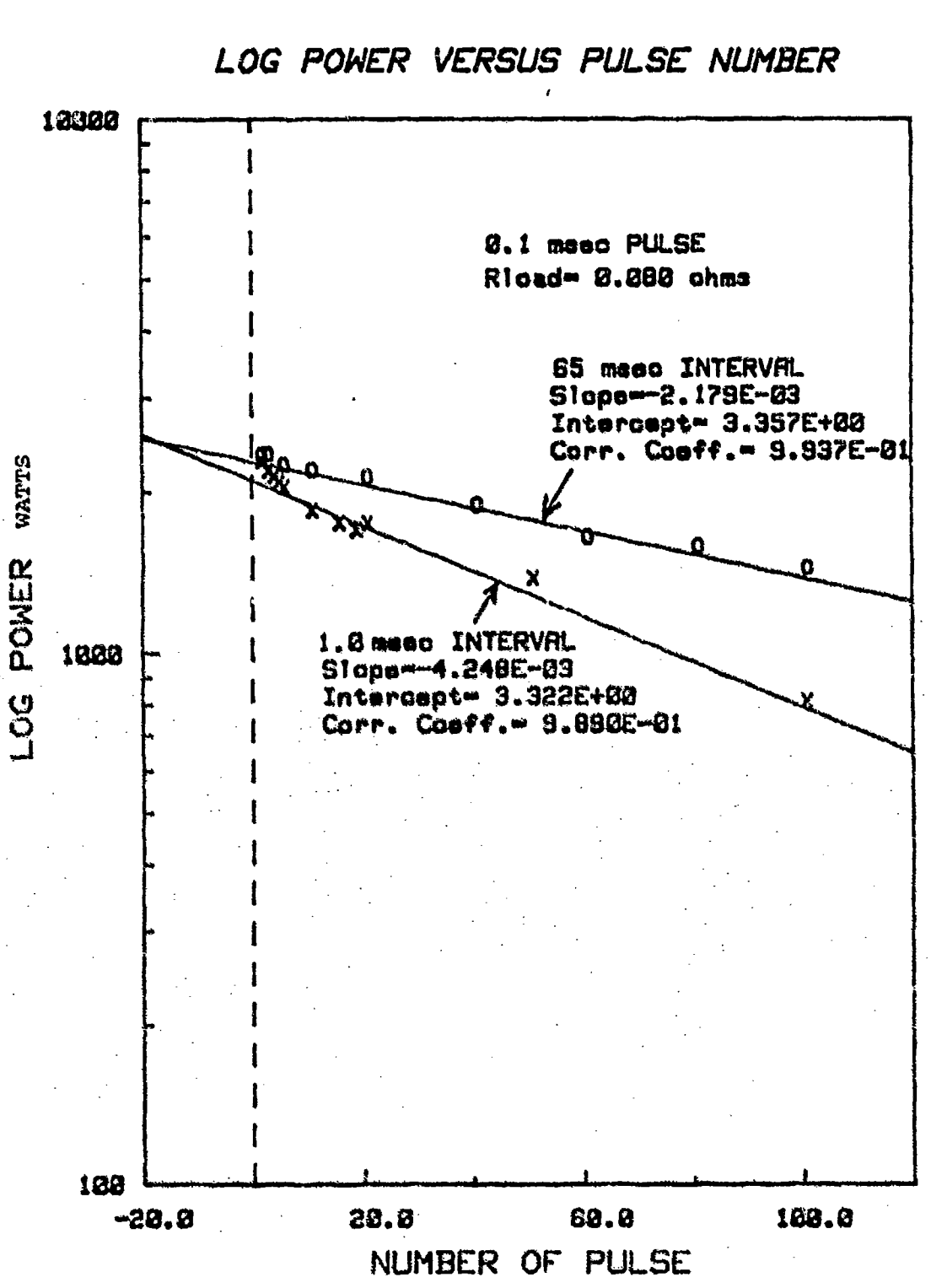

Fig. 13. Average pulse power in a series of 100 0.1 msec pulses

that the pulse width was sufficiently small. This characteristic may be particularly advantageous in applications where pulse count is more important than pulse energy.

III. BATTERY DESIGN

Present design considerations for the battery in the hybrid pulse power system are primarily discharge voltage and current, although other characteristics such as energy density, shelf life, operating temperature and safety have also played some role in the battery selection. Since the pulse power system may have more applications than one, our present choice is necessarily tentative.

Lithium-sulfur dioxide battery became the first choice for our present research after considering the various factors stated above. It then remained to determine the required voltage and current outputs, which in turn would be related to the duty cycle of capacitor's discharge.

A. Relationship between Duty Cycle and Voltage-Current Rating of the Battery

Within each duty cycle, in which more than one pulse can be delivered, charging of the capacitor can take place between consecutive pulses, or after the series of pulses has been delivered. The former case is more time efficient, but the latter is more easily analysed. Therefore the latter case will be considered first.

1. Mathematical Modeling

The governing mathematical relationships between various system parameters are as follows:

$$(1)\quad \frac{1}{2} C \left(V_{init}^2 - V_{rec}^2\right) = E, \text{ constant}$$

Here

E = energy consumed per discharge cycle
V_{init} = initial open circuit voltage (OCV) of the capacitor
V_{rec} = recovered OCV of the capacitor after the discharge
C = charge-storage capacitance

$$(2)\quad \frac{V_B(I) - V}{I} = R_c + r$$

where $V_B(I)$ is the output voltage of the battery,
V is the OCV of the capacitor during charge,
R_c is the shunt resistance in the charging circuit
r is the internal impedance of the capacitor, and
I is the charging current to the capacitor

$$(3)\quad I \leq I_{max}$$

where I_{max} is the maximum rated current for the battery (lithium-based)

$$(4)\quad \frac{V_{init}}{r_c} = G, \text{ a constant for a given operating voltage}$$

$$(5)\quad I = C \frac{dV}{dt}$$

Equation (4) is a characteristic of our ultracapacitor. For V_{init} = 36V, rC = 23 msec with the present ultracapacitor constructed. However further research on our capacitor technology can improve the values for these parameters.

2. Time Required for Charging

Charging of the capacitor is governed mainly by Eqs. (2) and (5). These equations are deceptive in that although they appear simple, V_B (I) is actually a non-analytic function of I*, and the equations in general must be solved numerically, subject to the boundary conditions:

(6) $t = 0$, $V = V_{rec}$

(7) $t \to \infty$ $V = V_B(I)$

Design calculation is simplified, however, by the approximation that

(8) $V_B(I) = V_B^0 - IR_B$

where R_B, the internal impedance of the battery, is assumed constant.

Substituting Eq. (5) into (2) and making use of Eq. (8) above, it is obtained that

$$(9)\quad V_B^0 = V + (R+r)\, C \frac{dV}{dt}$$

where $R = R_B + R_C$

Eq. (9) can be simply integrated to give a charging time of t_{chg} as follows

* $V_B(I)$ may also contain transients due to anodic passivation.

$$(10)\quad t_{chg} = (R + r)C \ln \frac{V_B^0 - V_{rec}}{V_B^0 - V_{init}}$$

$$= \left(\frac{R}{r} + 1\right) \frac{V_{init}}{G} \ln \frac{V_B^0 - V_{rec}}{V_B^0 - V_{init}}$$

by Eq. (4).

The shortest time for charging is thus achieved by maximizing the ratio of r/R, or with $R_c = 0$ and r is large enough that the initial charging current does not exceed I_{max}. By combining Eqs. (2), (3) and (8), the following constraint on the value of r is obtained.

$$(11)\quad \frac{V_B^0 - V_{rec}}{R + r} \leq I_{max}$$

Using Eq. (1) to eliminate V_{rec}, and eq. (4) to replace C by r, it then follows that

$$(12)\quad (V_B^{02} - V_{init}^2) - \frac{2\ ERG}{V_{init}} + \left(\frac{2EG}{V_{init}} - 2V_B^0\ I_{max}\right)(R+r)$$

$$+I_{max}^2\ (R+r)^2 \leq 0$$

clearly r is maximum when the expression above equals zero. Solving the resulting quadratic equation for R+r, one obtains a rather complex expression for $R+r_{max}$.

(13)

$$R+r_{max} = \frac{\left(\frac{EG}{V_{init}I_{max}} - V_B^0\right)^2 + 2\left(\frac{EGR}{V_{init}} - V_B^{02} + V_{init}^2\right) - \left(\frac{EG}{V_{init}I_{max}} - V_B^0\right)}{I_{max}}$$

However a simplification is afforded by the rather common occurrence that

$$2\left(\frac{ERG}{V_{init}} - V_B^{02} + V_{init}^2\right)$$

is much less than

$$\left(\frac{EG}{I_{max}V_{init}} - V_B^0\right)^2$$

because $E \sim 1/2\ C\ V^2_{init}$ and $V_{init}/I_{max} >> R$, so that the above expression for R+r reduces to:

(14)

$$R+r_{max} = \frac{R - (V_B^{02} - V_{init}^2)\ V_{init}/EG}{1 - \frac{V_B^0\ I_{max}V_{init}}{EG}}$$

The minimum time required to charge the capacitor between duty cycles is then given by Eq. (10) and the above as

(15)

$$t_{chg} = \frac{1 - (V_B^{02} - V_{init}^2)\ \frac{V_{init}}{EGR}}{\frac{V_B^0 I_{max}}{E} - (V_B^{02} - V_{init}^2)/ER} \cdot \ln \frac{V_B^0 - V_{rec}}{V_B^0 - V_{init}}$$

When $V_{init} = V_B^0$,

(16)

$$t_{chg} = \frac{E}{V_B{}^0 I_{max}} \ln \frac{V_B{}^0 - V_{rec}}{V_B{}^0 - V_{init}}$$

where $\dfrac{V_B{}^0 I_{max}}{\ln \dfrac{V_B{}^0 - V_{rec}}{V_B{}^0 - V_{init}}}$ can be regarded

as the average charging power of the battery. It can thus be be seen that the effective charging power depends not only on the characteristics of the battery, but on the capacitor's voltage as well.

3. Duty Cycle

The maximum duty cycle, in frequency units, of our hybrid pulse power system can be simply estimated as

$$\frac{1}{\text{Discharge time} + t_{chg} \text{ in Eq. (15)}}$$

However in practice, the duty cycle can be increased over the design value, by discharging the battery above the limit suggested by its supplier, and by partial charging of the capacitor between pulses. The actual limit on the duty cycle therefore remains to be investigated further in an experimental program. This is being planned.

B. Battery Specifications

Potential suppliers of lithium-sulfur dioxide batteries were contacted regarding general performance characteristics of this type of batteries as well as their availability. Presently a 24V nominal, 2 amp lithium-sulfur dioxide battery appeared suitable and would be available from Duracell within a short time period. With

$$V_B^0 = 24V \text{ and } I_{max} = 2 \text{ amp}$$

a resistive shunt was necessary for the charging of the current ultracapacitor constructed. Nevertheless Eq. (15) remains approximately correct with $V_{init} = 23V$. Then for the maximum depth of discharge, $E = 1/2C\ V_{init}^{0\,2} = 87$ Joules and $V_{rec} = 0$. The time required for charging is:

$$t_{chg} = 6 \text{ sec}$$

and the maximum duty cycle by design is

$$\frac{1}{1 \text{ sec} + 6 \text{ sec}} = 0.14 \text{ Hz}$$

given the battery supplies available. This corresponds to about 2 pulses/sec, still sufficient for the purpose of extrapolation.

The mathematical model used in the above design calculations remains to be verified, however, by comparison of experimental observation on the charging of the ultracapacitor by selected batteries with model prediction and this is planned. Practical theory lays the foundation for designing hybrid pulse energy systems to match specific applications.

IV. HYBRID PULSE ENERGY SYSTEM

A. Description

The hybrid pulse energy system combines the high power output of our ultracapacitor with the high energy density of a lithium battery to provide sustained bursts of energy at high power. The diagram in Figure 14 depicts this systems. To avoid conditions approximating short circuiting for the lithium battery, load resistor R_c was included in the charging circuit. The load resistance was selected to limit the battery's current to a maximum value, but could be removed if the condition specified by Eq. (11) was met.

The physical dimension of the battery is 6.2 cm x 11.2 cm x 12.7 cm. It is therefore much bulkier (about 85 times) than the ultracapacitor and its overall weight (including circuits with diodes and fuze) is 1 kg.

B. Charging Characteristics of the Battery/Capacitor Couple

The lithium battery was used to charge the ultracapacitor across various load resistors R_c to examine the validity of equations (9) and (10). By these equations the plot of ln $(V_B^0-V)/V_B^0$ against time should yield a straight line. Experimental results mostly bore out this prediction, as shown in Figures 15 and 16. However it was found that V_B^0 in the equations must be replaced by V_{max} given by

$$(17)\quad V_{max} = V_B^0 - i_{leak}\, R$$

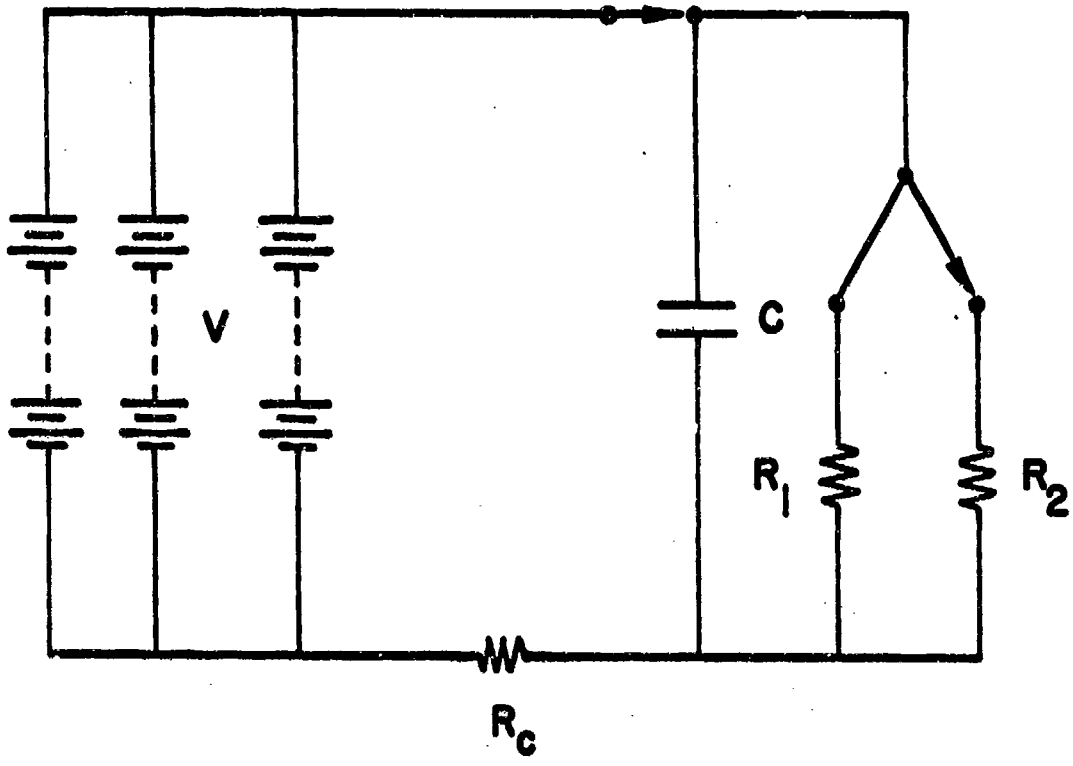

V = High-Energy Density Lithium Battery

C = PRI Ultracapacitor

R_c = Current-Limiting Resistor

$R_1 \gg R_2$, External Loads

Fig. 14. Hybrid Pulse Power System

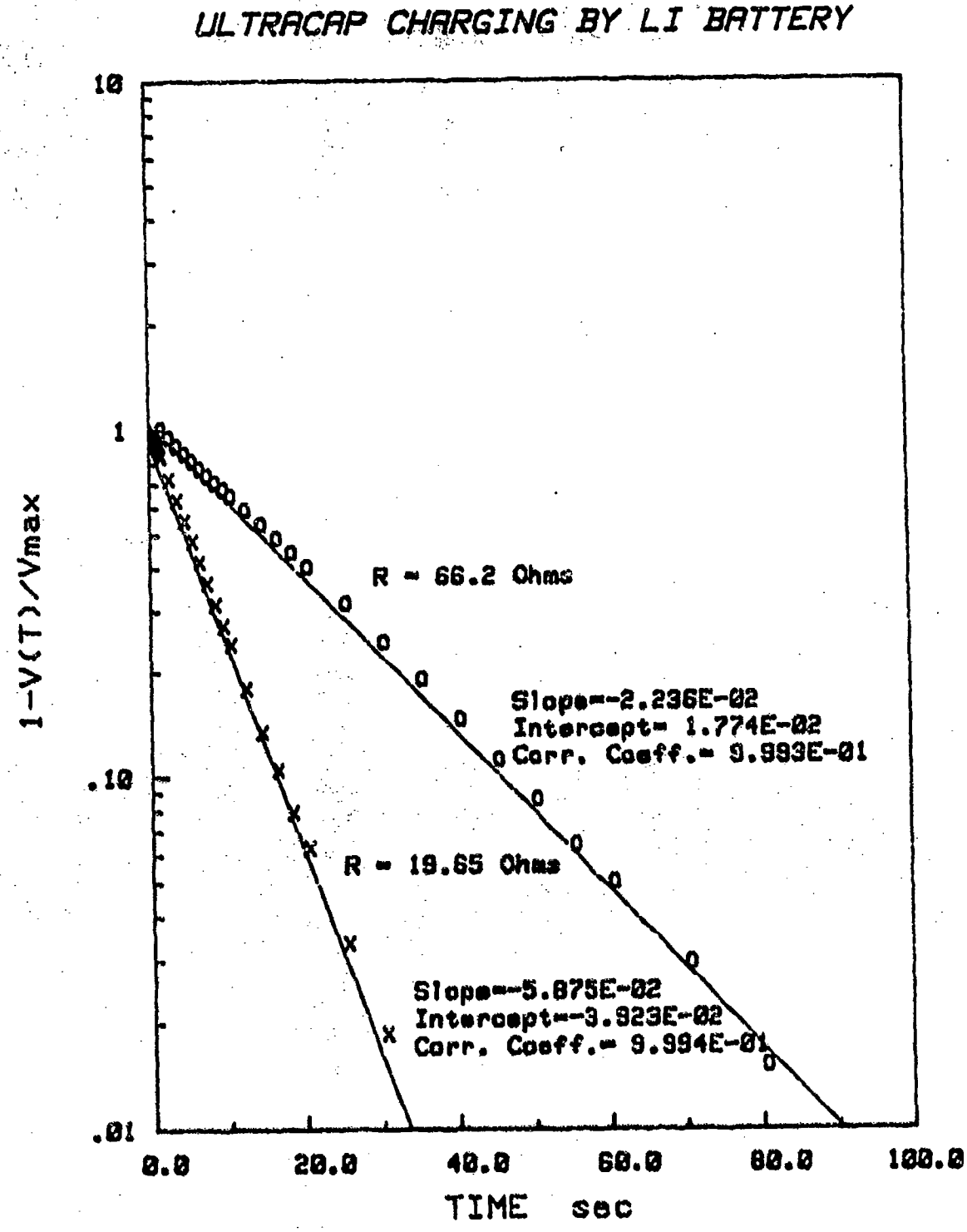

Fig. 15. Voltage on the Ultracapacitor during charging from rest by a lithium/SO_2 battery across various resistors R.

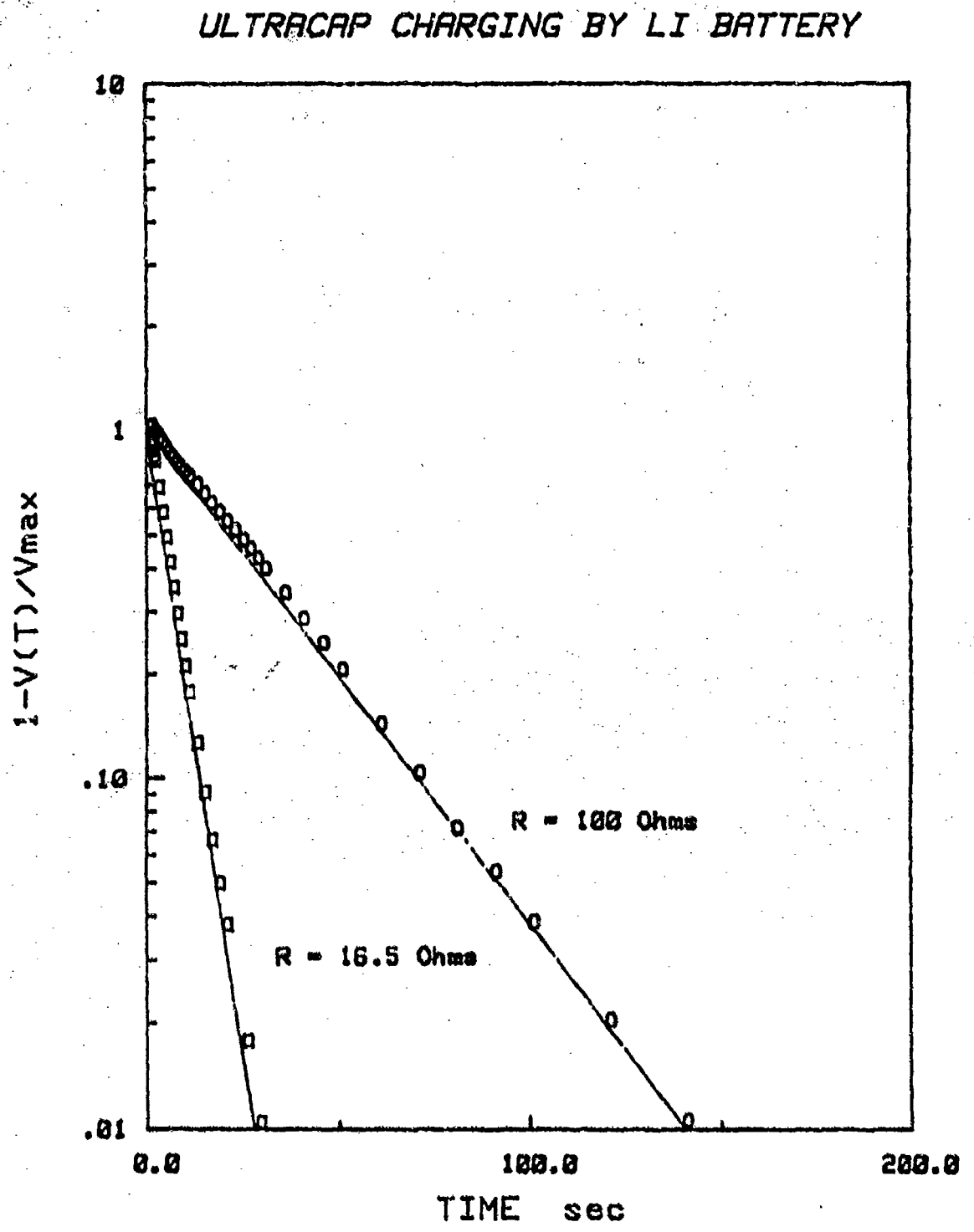

Fig. 16. Voltage on the Ultracapacitor during charging from rest by a lithium/SO_2 battery across various resistors R.

where i_{leak} is the leakage current. The inverse of the slopes of these plots gave time constants which, when plotted against R_c, should yield a straight line with the slope equal to the capacitance C of the capacitor and an intercept equal to$(R_B + r)C$. Figure 17 showed that this was indeed the case, with C = 0.285 F and R_B = 5 ohms. Hence the model equation did describe the charging behavior of the hybrid pulse energy system very well.

Equation (9) also indicates that the charging characteristics are functions of the total resistance R, but not on R_B and R_c independently. Hence the use of variable resistors in the charging circuit simulates the performance of batteries with different sizes, as described in the section below.

C. Duty Cycle Measurements

The duty cycle, defined as the number of pulses obtained from the hybrid pulse energy system per second, was determined experimentally by the following procedure. The capacitor was initially charged to a certain voltage V_{init}. It was then pulse discharged across a fixed load of 80 mohms for time intervals of 0.1, 1 and 3 msec corresponding to different pulse widths. Following the discharge in a single pulse, it was immediately recharged by the lithium battery to the initial voltage V_{init}. The time required for charging was recorded as t_{chg}, and the duty cycle was simply calculated as

$$\frac{1}{t_{chg} + \text{pulse width}}$$

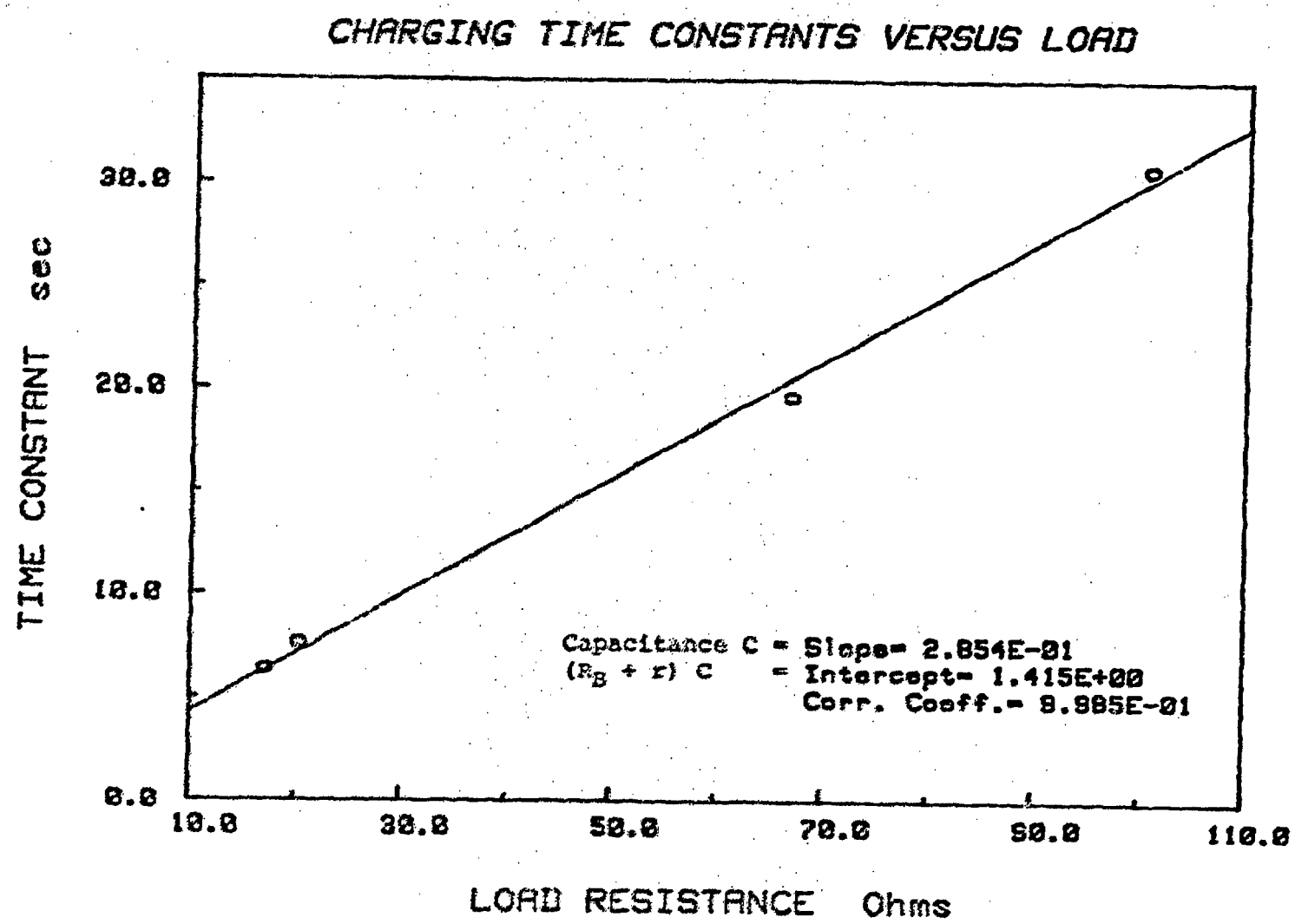

Fig. 17. Time constants for ultracapacitor charging across various load resistances R.

This duty cycle thus corresponds to an application in which the burst mode (a) of Fig. 9 is the desired output. The more complex output of burst mode (b) in the same figure is beyond the capability of existing equipment and hence not yet examined experimentally.

The performed experiments therefore measured the duty cycle as a function of V_{init} and pulse width. Moreover the maximum current from the battery during the charging portion of the cycle determines the minimum battery's size that would be required for the observed output from the pulse power system.

As an example, Figs. 18 and 19 show the typical results obtained with our duty-cycle measurements. Here the capacitor's voltage and current from the battery following a pulse discharge of the capacitor for 3 msec were monitored as a function of time. It can be seen that, due to relaxation phenomena in the capacitor after a discharge, and polarization phenomena in the battery, the charging characteristics deviate somewhat from that predicted by Eq. (9) and depicted in Figs. 15 and 16 earlier. However most of the deviations occur within the first 0.5 sec of charging, so that for duty cycle considerably less than 2 Hz, the rather simplistic model presented in Section III. A.1 remains a good approximation.

For duty cycle of 2 Hz or above, the present model still predicts the experimental trends, as summarized in Figure 20. The results clearly indicate that decreasing the voltage on the

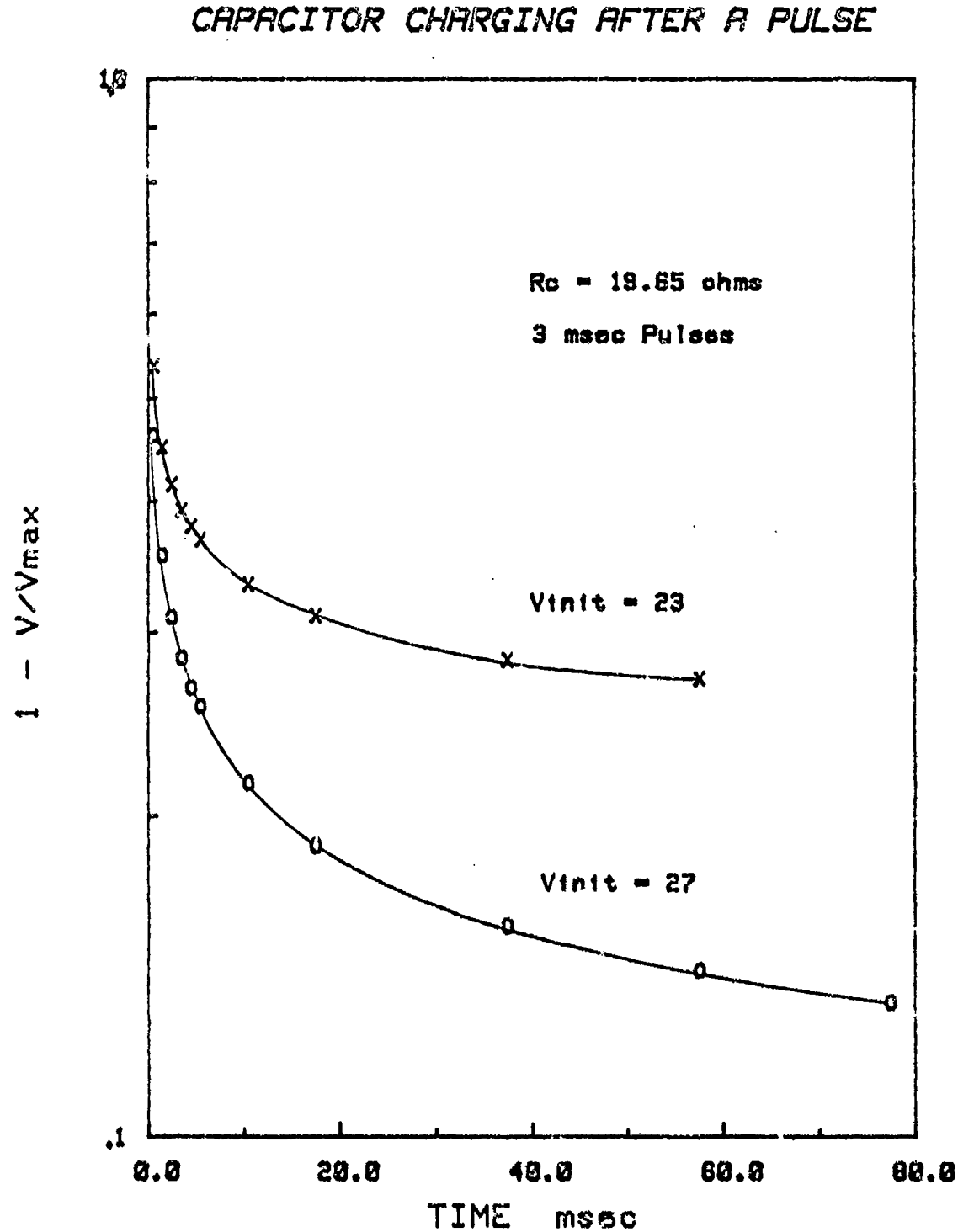

Fig. 19. Transient behavior of ultracapacitor's voltage during charging immediately after a pulse discharge.

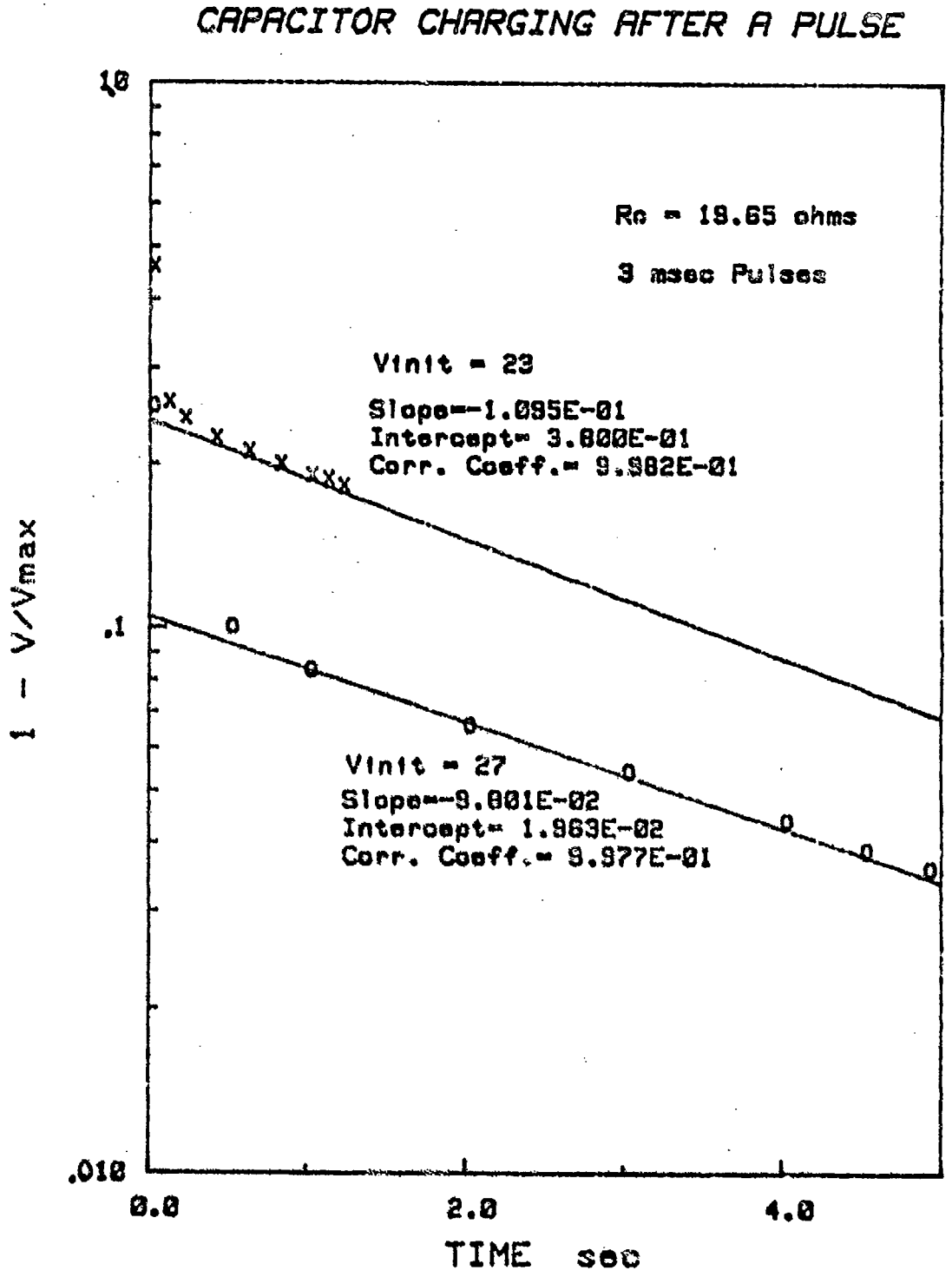

Fig. 19. Long-time behavior of ultracapacitor's voltage during charging immediately after a pulse discharge.

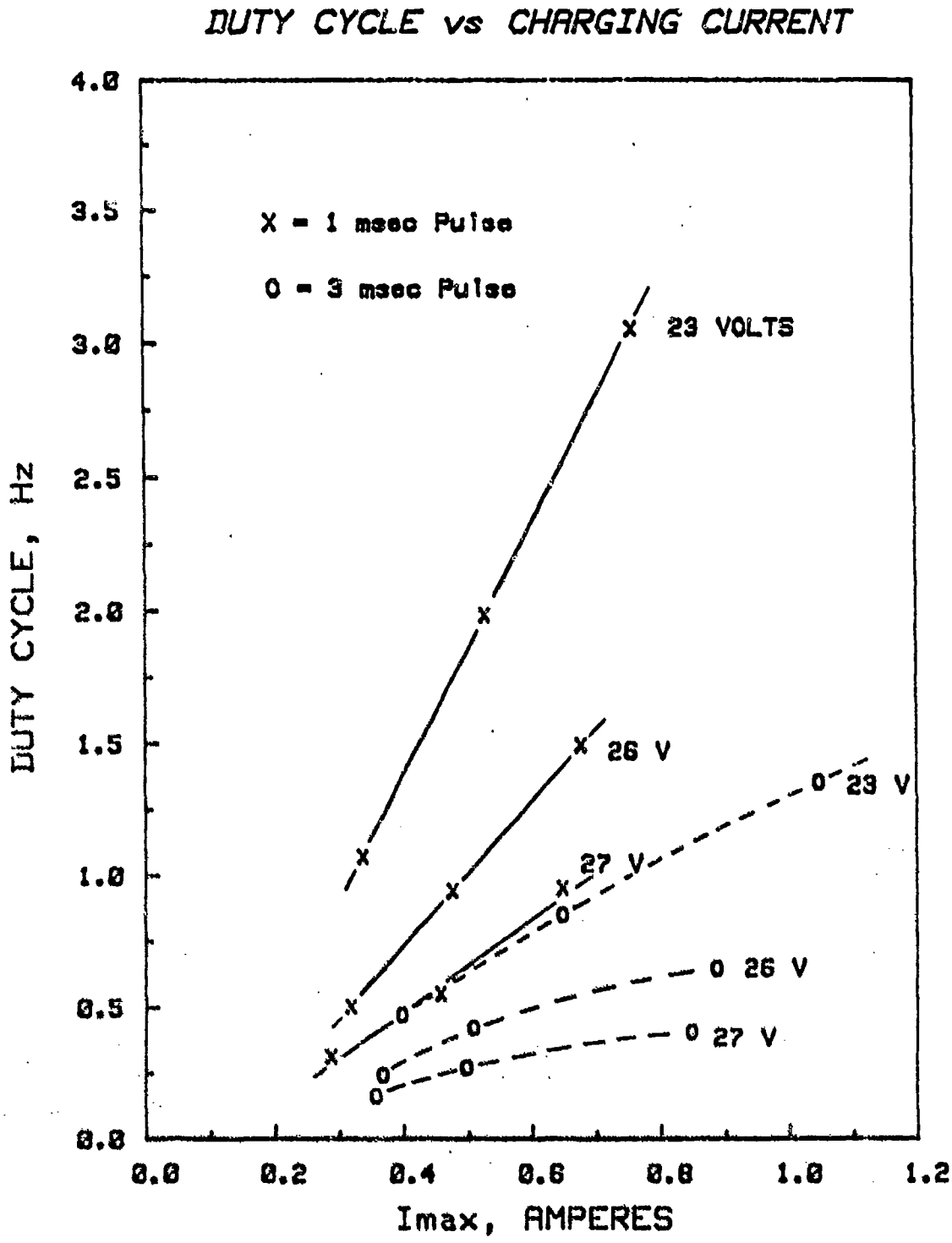

Fig. 20. Dependence of the duty cycle of the prototype hybrid pulse power system on various system parameters.

capacitor has a beneficial effect on the duty cycle. In addition, the duty cycle is proportional to maximum current from the battery for 1 msec pulses output, as predicted by Eq. (16). However for 3 msec pulses the model did not fare as well, probably as a result of the longer relaxation time for the capacitor following a 3 msec discharge versus 1 msec.

D. Performance Projections

With further research and development, the performance level of the hybrid pulse power system can be raised orders of magnitude above that demonstrated for the prototype system in this work. Important applications which require hundreds of megawatts of burst power such as rail gun can enjoy the advantages of our pulse power system, assuming that ultracapacitors of a much increased size can be fabricated without significant performance degradation. Furthermore, improvements in the energy and power densities of the ultracapacitor or battery can lead to systems of reduced sizes and weights.

Extrapolation of the hybrid pulse power system first to one capable of delivering 100 MW bursts of energy can be performed by assuming no change in the energy and power densities of both the capacitor and the battery. The following relationships can be shown to apply.

Battery size $\propto$ Maximum charging current

Charging current $\propto$ Size of capacitor

Size of capacitor $\propto$ Burst power

The weight of the battery can thus be extrapolated from the experimental results given in Figure 20, and then plotted in Figure 21 as a function of duty cycle. It can be seen that, in general, lowering the voltage on the capacitor can reduce substantially the weight of the battery. Although the data correspond to some rather atypically large lithium battery packs, it must be emphasized that they do not necessarily represent real situations. For example it may well be that the burst model (b) shown in Fig. 9 describes the actual application. This situation, however, has not been examined in detail due to limitations with existing test equipment. Nonetheless it can be deduced that here the duty cycle for charging, which determines the battery's weight, may be quite independent of the duty cycle for pulse discharges which determines the capacitor's weight. This feature, peculiar to high-energy density capacitor, can offer significant reduction in system's size and weight in certain applications.

As an example, an application involving a pulse frequency of 2 Hz but with a rest interval of 10 sec between series of pulses would require a battery weighing about 20,000 kg if recharging were needed between consecutive pulses, as in burst mode (a) of Fig. 9. However with the ultracapacitor operating in burst mode (b) charging could occur during the rest interval, resulting in a battery weighing no more than 12,000 kg, calculated based on Eq. (16) and the assumption of maximum depth of discharge in each series of pulses.

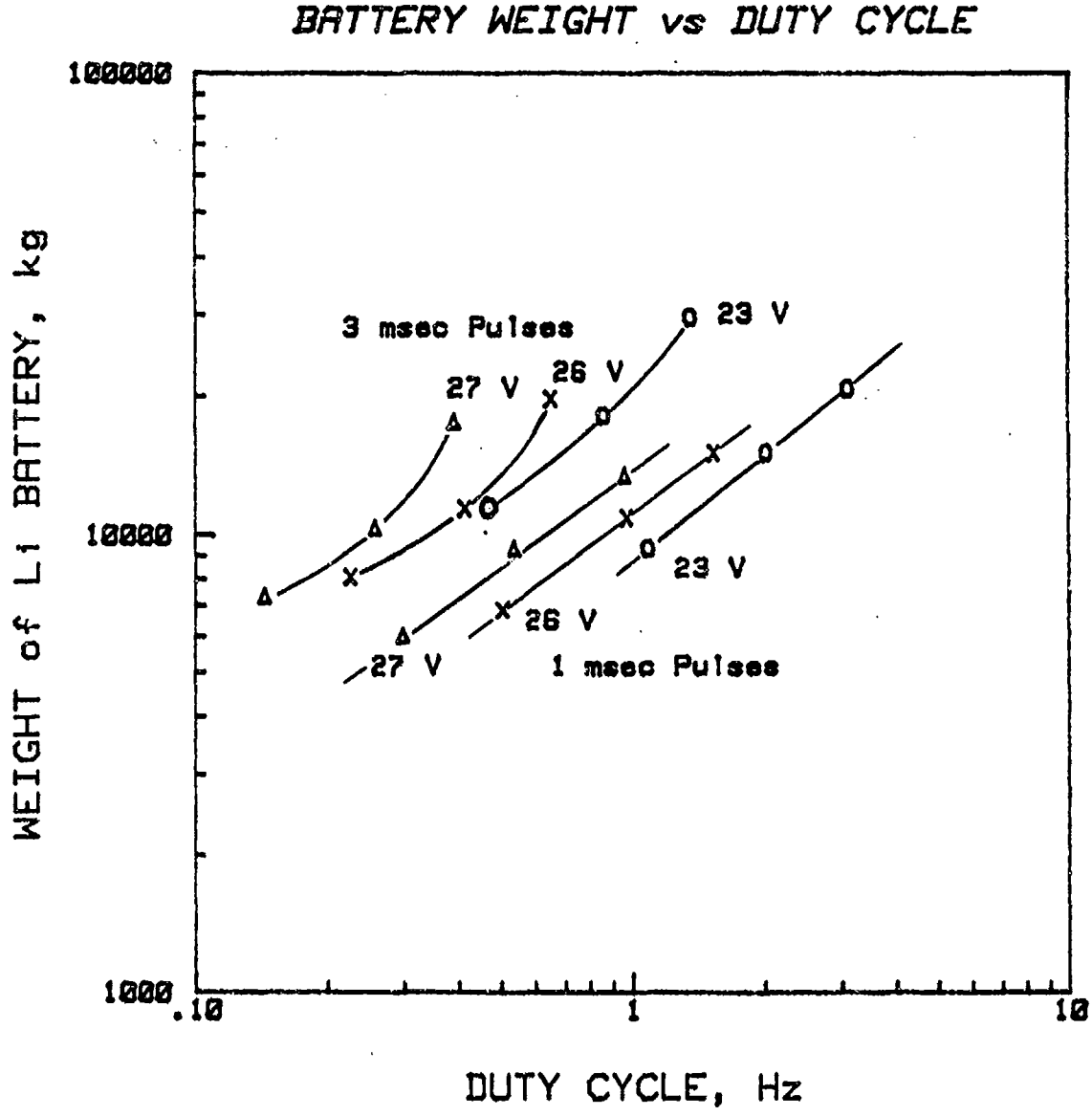

Fig. 21. Projected weights of lithium/SO_2 battery in hybrid pulse energy system capable of delivering pulses at 100 MW peak power.

The weight of the capacitor, which can be calculated to be 1400 kg based on a power density of 72 kW/kg, is not insignificant though it may appear small compared to the battery. Recognizing that the size of the battery may be reduced with other types of batteries, such as Silver oxide-Zinc, an independent consideration must be given in an exploratory research program to reducing the capacitor's weight.

Table 1 summarizes the state of art and near term performance goals of the ultracapacitor. With a power density of 800 kW/kg, the weight of the capacitor can be reduced further to 125 kg, or 1250 kg for burst power of one gigawatt. This high performance for the ultracapacitor is believed realizable through the minimization of the interelectrode gap and the reduction of the electrode thickness in the stack comprising the main body of the ultracapacitor.

The size of the ultracapacitor may in certain applications be governed by its energy rather than power density as previously assumed. This applies when the burst power to useful energy (P/E) ratio of the capacitor in burst mode (b) of Fig. 9 exceeds the same ratio required in a duty cycle. As an example, a series of 1000 1 msec pulses at peak power of 100 MW requires a useful energy of about 55 MJ (peak to average power in a pulse approximately 1.8 by Fig. 4 and 7). The P/E ratio is therefore 1.8 sec^{-1} but the expected ratio for the ultracapacitor is about 90 sec^{-1} as seen in Fig. 12. The weight of the capacitor thus

TABLE I
PRI ULTRACAPACITOR - WHERE IT IS AND WHERE IT CAN GO

	SOA	Far Term* SOA
Energy Density		
kJ/kg	6.4	20
MJ/M^3	20	64
Power Density		
kW/kg	72	800
MW/M^3	220	2500
Voltage	84	> 1kV †
Maximum Current Density (A/cm^2)	27	66

* Based on component parameters below.
1 mil interelectrode gap. 1 mil Ti substrate.

† Cells can be stacked to attain any voltage.

CURRENT PHYSICAL PARAMETERS OF PRI ULTRACAPACITOR COMPONENTS

Ti Substrate Density	4.5 gm/cc
Mixed Oxide Coating Density	3.4 gm/cc
Effective Sheet Resistance in a Unit Cell	
Interelectrode Gap (Electrolyte + Separator = 1 mil)	7.98 $m\Omega\text{-}cm^2$/cell
Two 0.65 mil thick mixed-oxide layers per unit cell	9.24 $m\Omega\text{-}cm^2$/cell
Specific Electrode Capacitance	1.5 G/cm^2

becomes

$$\frac{55 \text{ MJ}}{0.64 \text{J/gm}} = 86{,}000 \text{ kg}$$

as opposed to 1400 kg calculated earlier. Increasing the stored energy density from 6.4 kJ/kg to 20 kJ/kg should lead to a proportional increase in useful energy, thus reducing the size of the capacitor to 27,500 kg.

Further advances may yet be achieved through alteration of the charge-storage coating on the ultracapacitor electrode to increase its specific capacitance. One approach involves the use of thicker oxide coatings on the electrode to increase its capacitance to as much as $5F/cm^2$, resulting in an energy density of

$$\frac{1/2CV^2}{\text{weight}} = \frac{1/2 \text{ (2.5 F/cm}^2\text{-cell) (1.2 volt/cell)}^2}{\text{(0.00254 cm x 4.5 g/cc + 50mg/cm}^2\text{)}} = 30 \text{ kJ/kg}$$

assuming a 1 mil Ti substrate with a density of 4.5 g/cc and a specific capacitance for the coating of 0.2 F/mg-side. This means a useful energy density of about 3 kJ/kg, and a capacitor weighing 18,000 kg for 1000, 1 msec pulses at 100 MW peak power.

Other approaches through basic materials research may lead to quantum jumps in both stored and useful energy densities. Minimizing the discrepancy between the two density parameters reduces the weight of the above capacitor to 1800 kg. The surface area available from our present mixed oxide materials is about 120 m^2/gm. High surface area, conductive materials do exist (e.g. activated carbon) with surface areas >1000 m^2/gm. If such a material could be developed and affixed to a substrate while maintaining its surface area, an energy density >200 kJ/kg could be the new technology limit, enabling the use of only capacitors which can store enough energy to deliver all the pulses needed for a burst power application without recharging by batteries. In this scenario only a low power battery is needed to replenish the charge lost in the capacitor due to leakage current.

Even if high battery power is needed for charging the capacitor, batteries that can operate at current densities greatly exceeding that of the nonaqueous lithium battery (recommended current density at 5 mA/cm^2) are available. An aqueous lithium battery recently developed by PRI and Gould's Ocean System Division can operate at current density as high as 1 A/cm^2. This means that the size of the battery can be reduced to become comparable to that of the capacitor, if battery power is the only consideration in the design of the hybrid pulse power system. The actual weight of the system must therefore be determined on a case by case basis for specific applications.

V. CONCLUSION AND SIGNIFICANCE

Hybrid pulse power systems can be assembled to meet a variety of continuous and burst power requirements. Increased flexibility is afforded by the use of a recently developed, high-energy density capacitor (the PRI ultracapacitor) which is capable of delivering multiple bursts of energy at high power (>100 at 100 MW/m^3) before requiring recharge. Consequently pulses can be delivered at a broad range of time intervals (down to milliseconds) based on demands. Furthermore the average power in a pulse is approximately 50% of the peak power, compared to much less for conventional capacitors.

Some discrepancies are observed between the stored energy density, and useful energy density, the latter being somewhat less. Further research on our capacitor technology can minimize these differences, as well as to reduce dramatically the bulkiness of the capacitor in applications requiring gigawatts of burst power.

A basis for the optimal design and performance projections for the hybrid pulse power system was established. Parametric relationships between pulse width, pulse interval, load resistance, initial voltage and discharge power for the ultracapacitor were investigated and found to be readily correlated. The discharge power was found to be proportional to initial voltage to the 1.8^{th} to 2^{nd} power, and was maximum at load resistances slightly greater than that of the ESR of the capacitor.

In a series of pulses, the power decreased exponentially, with the decline being more gradual with larger intervals between pulses. A consequence was that there was a tradeoff between useful power and energy density.

A model was developed for the hybrid pulse power system and found to be quite satisfactory for low duty cycle and small pulse widths. It also predicted the trends of the experimental data very well. Generally the limit on the duty cycle is raised by increasing the current capability of the battery, decreasing the output voltage of the capacitor (relative to that of the battery), and using pulses of a reduced duration. These results were obtained with a single pulse in each duty cycle but the same conclusions should apply for multiple pulses per cycle.

Extrapolation of the weights of the lithium battery required for an assumed application showed that they were substantially larger than the capacitor. Alternate batteries with higher power densities should be considered for optimizing system's weight when burst power is the primary goal. In another approach the capacitor can be used to store enough energy to meet all burst power requirements, in which case a high-energy density battery will be useful for replenishing the charge lost in the capacitor due to leakage current.